Geomorphology 241 (2015) 175–191

Contents lists available at ScienceDirect

Geomorphology

journal homepage: www.elsevier.com/locate/geomorph

Longshore variability of beach states and bar types in a microtidal, storm-influenced, low-energy environment

N. Aleman [a,*], N. Robin [a], R. Certain [a], E.J. Anthony [b], J.-P. Barusseau [a]

[a] Perpignan University, Centre Européen de Formation et de Recherche sur les Environnements Méditerranéens (CEFREM), UMR5110, 52 Avenue Paul Alduy, 66860 Perpignan Cedex 9, France
[b] Aix-Marseille University & Institut Universitaire de France, Centre Européen de Recherche et d'Enseignement des Géosciences de l'Environnement (CEREGE), UM 34, Europôle Méditerranéen de l'Arbois, BP 80, 13545 Aix-en-Provence Cedex 4, France

ARTICLE INFO

Article history:
Received 18 September 2014
Received in revised form 10 March 2015
Accepted 15 March 2015
Available online 17 April 2015

Keywords:
Beach states
Bar types
Geological context
LiDAR
Nearshore bars
Dean parameter

ABSTRACT

Beach classification models are widely used in the literature to describe beach states in response to environmental conditions. These models were essentially developed for sandy barred to barless beaches in micro- to meso-tidal environments subject to moderate to high wave energy conditions and have been based on field studies over limited stretches of coast. Here, we further interrogate the performance of the Australian beach classification scheme by analysing beach states and corresponding bar types on a regional scale in a storm-influenced, low wave-energy, microtidal environment, using a large and unique spatial and temporal dataset of supra- and subtidal beach morphology and sedimentology. The 200 km-long coast of the Gulf of Lions in the Mediterranean consists of quasi-continuous sandy beaches with a well-developed double sandbar system. All the reported classical beach states were observed on this coast, from reflective to dissipative, along with two more unusual states: the rock platform-constrained beach state which is associated with bedrock outcrops, and the non-barred dissipative beach state which is more commonly found in large tidal-range settings. LiDAR bathymetry shows that the transitions between beach state zones are marked mainly headlands but transitions also occur progressively along stretches of continuous sandy beach. The longshore distribution of beach states and associated bar types on a regional scale can be related to the variability of hydrodynamic conditions (wave incidence and energy) and sediment characteristics (particle size). However, the influence of these parameters on beach state seems to be largely controlled by the geological context such as the presence of a river mouth, headland or rock platform. Finally, we assessed the ability of the parameter Ω, commonly used to characterise beach states, which combines wave characteristics and sediment fall velocity, to predict the observed beach states and bar types using a very large set of hydrodynamic and sedimentary data. Our results, based on high frequency spatial sampling, show that the fall velocity of the subtidal sediment coupled with wave statistics one month prior the observed beach state strongly improved the predictive power of the parameter Ω.

1. Introduction

Beaches play a major environmental role as buffers of wave energy and storms (Wright and Thom, 1977). One major focus of coastal research is to relate environmental parameters to beach morphological change (Cowell and Thom, 1994). Many beach studies assume that a system can move towards a state of dynamic equilibrium under steady forcing conditions (wave climate, tidal regime and beach sediment characteristics), following the morphodynamic postulate of Wright and Thom (1977). Consequently, various conceptual beach models backed, or not, by simple semi-quantitative parameters have been proposed, enabling a better understanding of beach morphological systems (Sunamura and Takeda, 1984; Wright and Short, 1984; Lippmann and Holman, 1990; Short, 1991, 1992; Masselink and Short, 1993; Short and Aagaard, 1993; Levoy et al., 1998; Scott et al., 2011). These models also throw light on other aspects of beach dynamics, such as variations in beach volume, basic hydrodynamic signatures and sediment movement. Wright and Short (1984) developed a now commonly used empirical model that classified beach states according to the parameter Ω (Dean, 1973), also commonly known as the dimensionless fall velocity, given by: $\Omega = H_b/W_sT$ where H_b represents wave breaker height, W_s the sediment fall velocity, and T the wave period. Wright and Short (1984) suggested that Ω must be less or equal to 1 for a beach to be fully reflective, and greater or equal to 6 in order for it to be in a fully dissipative state. Intermediate beach states tend to occur for Ω between 1 and 6, and are characterised by variable nearshore bar systems: Low Tide Terrace (LTT), Rhythmic Bar and Beach (RBB), Transverse Bar and Rip (TBR) and Longshore Bar-Trough (LBT). Later, Masselink and Short (1993) proposed a beach state model for meso- and macro-tidal beaches using the Relative Tidal Range (RTR) and established corresponding characteristic values of Ω. Other dimensionless indices (surf similarity

* Corresponding author. Tel.: +33 468662057.
E-mail address: nicolas.aleman@univ-perp.fr (N. Aleman).

http://dx.doi.org/10.1016/j.geomorph.2015.03.029
0169-555X/

parameter (Battjes, 1974) and surf scaling parameter (Guza and Inman, 1975)) based on wave and beach slope characteristics are less used. The Wright and Short (1984) model has been widely used to elaborate regional or local beach state classification schemes (e.g., Short, 1992, 2006; Calliari et al., 1996; Benedet et al., 2004b; Costas et al., 2005; Castelle et al., 2007; Sénéchal et al., 2009; Price and Ruessink, 2011). Most beach state studies have been conducted on sandy beaches dominated by moderate to high wave conditions, and only limited research has been undertaken on beaches subject to low wave energy, which have been shown to respond very differently to changing wave conditions (Hegge et al., 1996; Jackson et al., 2002; Costas et al., 2005; Gómez-Pujol et al., 2007).

Whatever the wave-energy context, several studies have found low correlations between the predicted and observed beach morphologies (Wright et al., 1987; Sanderson and Eliot, 1999; Jackson et al., 2005; Gómez-Pujol et al., 2007; Grasso et al., 2009; Loureiro et al., 2013). This poor relationship has been justified by the weakness of the discriminatory capacity of the parameter Ω under certain conditions. Indeed, the original sediment and wave parametric characterisations of the beach state model of Wright and Short (1984) were essentially drawn from swell-dominated beaches in Australia enclosed between bedrock headlands and commonly dominated by cross-shore sand exchanges between the beach and the nearshore zone. This can be a source of discrepancy when Ω is deduced in other types of wave environments. The predictive power of sediment-wave parameters to characterise beaches has been questioned (Anthony, 1998). In some circumstances, incident wave heights and periods may vary temporally and alongshore, probably as a result of harmonic decoupling and wave reforming over a complex changing nearshore morphology, coastline orientation or seasonal effects. Median grain size and mean settling velocity may also vary markedly over time and no standardized rules on sediment sampling locations are clearly recommended. Such considerations of procedure have received little attention but do affect the representativeness of sediment-wave parametric combinations in relation to the beach environment (Anthony, 1998; Scott et al., 2011; Short and Jackson, 2013). Recently, geological setting has been highlighted as another controlling factor of beach states, notably through headlands, rock platforms, sediment supply and accommodation space (e.g., Cooper and Pilkey, 2004; Jackson et al., 2005; Vousdoukas et al., 2005; Short, 2006, 2010; Backstrom et al., 2009; Jackson and Cooper, 2009; Muñoz-Perez and Medina, 2010; Loureiro et al., 2013). Notwithstanding these various reservations, Ω has been successfully used recently in equilibrium models predicting shoreline evolution (Davidson et al., 2013; Splinter et al., 2014).

Consequently, the discrimination and influence of each control parameter are difficult to determine and many more case studies from contrasting environments are needed for a better morphodynamic characterisation of beach states. In particular, a key element in mapping and understanding the spatial representation of bar-beach states and their longshore variability is that of having accurate 3D data and on a large spatial scale, and over the long term, in order to bring out equilibrium beach states. Previous observations of beach states are commonly based on aerial photographs, which have the advantage of good spatial extension (regional scale) but limited 3D restitution, as well as sporadic topo-bathymetric data (DGPS, video) of low spatial extension. These limitations have probably encouraged the use of the parameter Ω in spite of the limitations highlighted above. Furthermore, many of the reported case studies in the literature are beach sites with well-marked boundaries (headlands, rocks, reef, islets or islands) inducing a short average beach length and individual beach state compartments that can be more readily characterised (Jackson et al., 2005; Short, 2006; Gómez-Pujol et al., 2007; Klein et al., 2010; Scott et al., 2011; Loureiro et al., 2013). The spatial transition between bar-beach states on long open beaches without such boundaries has been poorly documented.

This paper complements recent work on the typologies of nearshore bars in the study area (Aleman et al., 2011), and analyses spatial beach state variability along 200 km of microtidal low-energy sandy coast in the western Gulf of Lions, France (Fig. 1). The main approach adopted here lies in the use of very high-resolution 3D LiDAR topo-bathymetric data, which have the advantage of representing beach states and especially their transitions with good accuracy on a regional scale compared to traditional technologies (bathymetric and video survey). In addition to the LiDAR data, the results of previous studies and input from aerial photographs have also been used to obtain a robust determination of modal beach states. The objectives are to: (1) determine the range of modal beach states associated with a suite of more or less complex bar morphologies with respect to classifications proposed in the literature, and illustrate and describe the longshore transitions between the different beach states; (2) identify the role of geological constraints in influencing beach states and their transitions, as well as the influence of engineering structures on such states and transitions; and (3) assess the influence of cross-shore distribution of sediment size and wave climate variability on the performance of Ω in a microtidal low-energy sandy coast.

2. Study area

The study area, located along the Languedoc-Roussillon coast of the Gulf of Lions is a Holocene curvilinear lowland unit stretching over 200 km and comprising narrow sand barriers that isolate several lagoons (Fig. 1). Since the 1970s, large tourist complexes have been built on many of these barriers which are bound by rocky headlands, river mouths and several harbours. The upper shoreface displays a succession of 1 to 3 bars and troughs that vary in shape (linear or crescentic) and depth from one site to another (Barusseau and Saint-Guily, 1981; Aleman et al., 2011) (Fig. 1A).

Aleman et al. (2011) defined the various bar types (Dissipative (D), Longshore Bar-Trough (LBT), Transverse Bar and Rip (TBR), Rhythmic Bar and Beach (RBB), Low Tide Terrace (LTT) and Reflective (R)) on the basis of the model proposed by Wright and Short (1984), and mapped their distributions, pointing out different intermediate and complex bar types. In the southern part (40.5 km of coastline), the inner bar (IB) and the outer bar (OB) are crescentic. The inner bar alternates between the TBR and RBB types, with many transitional TBR/RBB shapes. In the central part (78.3 km), the inner bar is mainly crescentic RBB or TBR with 47% of oblique configurations. The outer bar displays mainly a straight configuration with LBT or D morphologies. The northern part (69.4 km) is different from the other two. To the west, the system exhibits a double straight bar configuration (LBT or D). The bar system then displays one or no bar to the east.

The nearshore slope pattern along the Gulf of Lions is depicted in Fig. 2. The upper shoreface (including the nearshore bar system) shows significant longshore variation at local and regional scales (between 0.37° and 2.47°) due to the presence of large bars and the geological setting (river-mouth pro-deltas or bedrock outcrops) as well as anthropogenic structures (harbours or coastal defences). The lower shoreface (from the outer edge of the bar system to 1 km offshore) and the entire shoreface (from the shoreline to the offshore limits of LiDAR detection at about −20 m depth) are very similar between 0.08° and 1.35°. Gentle slopes (0.1° to 0.2°) correspond to zones where bedrock outcrops occur (southern part of the coast near the Pyrenees, Cape Leucate, and the subtidal rock platforms of Aresquiers and Palavas-Maguelone). Overall, the three parts of coast exhibit the same longshore northward decreasing, then increasing, trend in slope (Fig. 2). In the southern part, the gradient of the entire shoreface varies between 0.74° and 1.32°, whereas in the central and northern part it oscillates around 0.46°. A net decrease in slope occurs at Cape Leucate (Fig. 2). Changes in other environmental parameters such as bar patterns or sediment characteristics are also observed in the vicinity of the cape. Generally, a slope increase occurs on the right side of coastal river mouths (except for the Orb and Hérault in the central part), updrift of Capes Leucate and Agde, and at the distal end of Espiguette spit on the

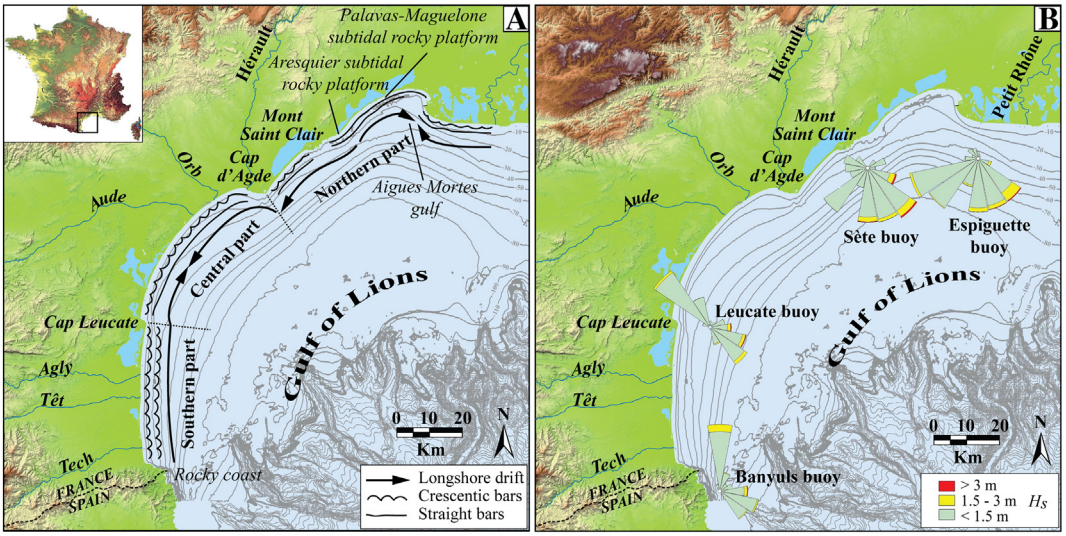

Fig. 1. Map of the Gulf of Lions showing: (A) the general pattern of bars and longshore drift, and (B) wave conditions and directions. Adapted from Certain, 2002.

Rhône delta (Fig. 2). Conversely, the slope decreases downdrift of both capes. The mean depth of wave closure on this coast is around −6 and −8 m (Durand, 1999; Sabatier et al., 2004). In the northern area, the substratum outcrops at depths of −5 to −10 m forming a wide rock platform. Consequently, the sedimentary stock is limited and close to the shore. Geophysical data show that sand thickness does not exceed 4 m, and sometimes bedrock crops out on the inner and outer troughs of bars (Certain et al., 2005b). An estimation of the sediment budget for this coast over the period 1984–2009 shows that erosion has been dominant, with a volume loss of $-30.2 \pm 4.2 \times 10^6$ m^3 (Brunel et al., 2014).

The Gulf of Lions is a microtidal, wave-dominated environment. The tidal range is very low (<0.30 m at mean spring tides). Nevertheless, large variations in water level can occur in response to wind forcing and atmospheric pressure fluctuations. Set-up can attain 1 m near the shore (Certain, 2002) under the combined action of storm surge and waves. Two wind orientations prevail: NW offshore winds (60% of the time) and E to SE onshore winds (30% of the time) (Casanobe, 1961; Person, 1973; Cattaliotti-Valdina, 1978; Mayençon, 1992). Significant wave heights (H_s) impinging on the coast are generally low (H_s < 0.3 m for 75% of the time and H_s < 1.5 m for 94%), with peak periods (T_p) between 5.7 and 6.3 s. Wave heights larger than 3 m are observed less than 1% of the time, with T_p between 5 and 10 s. Wave heights can reach 7 m during exceptional storms (1982, 1997 and 2003) with periods around 12 s. The maximum wave heights (H_{max}) at Sète are 5, 7.8 and 9 m for return periods of 1, 10 and 100 years, respectively (L.C.H.F., 1984). Waves from SW to N are generated by offshore winds and are low, whereas waves from E to S are generated by onshore winds and are the most energetic (Fig. 1B). Table 1 shows the temporal variation of wave characteristics assessed from the monthly and annual wave data for four stations along the Gulf of Lions. Spring and summer (April–September) are characterised by low waves (0.42–0.60 m monthly mean height) with few major storms (3.67 m max height at Leucate and Sète). The standard deviation is low, between 0.25 and 0.43 (Table 1). July, August and September are the months with the lowest waves (0.42–0.50 m monthly mean height). The autumn and winter period (October–March) displays the highest waves, although the monthly mean height is not much higher (0.76–0.90 m). During this

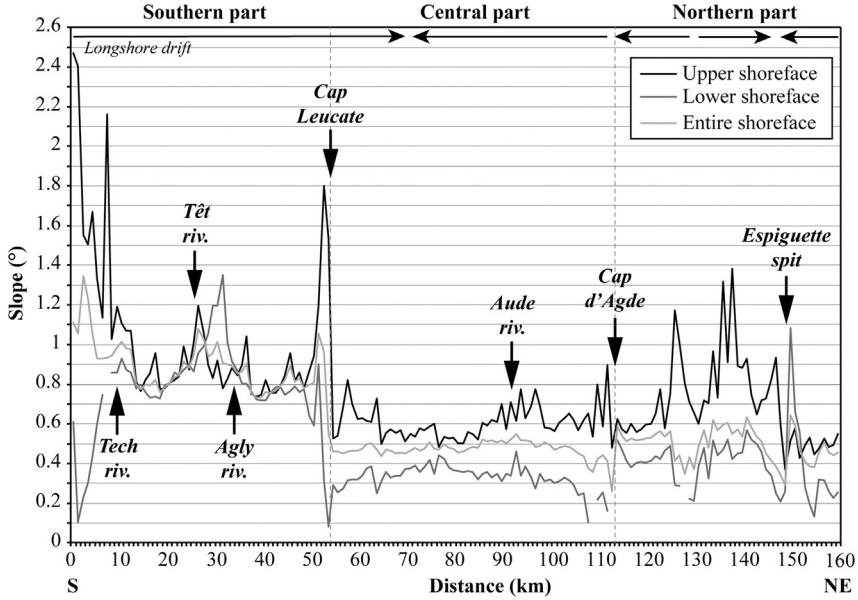

Fig. 2. Longshore evolution of the slope for the upper shoreface, lower shoreface and entire shoreface (up to 1 km offshore).

Table 1
Annual and seasonal statistics of significant wave height (H_s) in the Gulf of Lions for the four wave buoys (4–10 year record period). *N*: number of records; *Min*: minimum significant wave height; *Max*: maximum significant wave height; $\overline{X}$: mean significant wave height; σ: standard deviation of significant wave height; 0–1.5 m: percentage of wave height between 0 and 1.5 m; 1.5–3 m: percentage of wave height between 1.5 and 3 m; >3 m: percentage of wave height higher than 3 m. JFM: January, February and March (winter); AMJ: April, May and June (spring); JAS: July, August and September (summer); OND: October, November and December (autumn).

Buoy	Location	Period of records	Statistical period	N	H_s (m)	$H_s max$ (m)	σH_s (m)	Tp (s)	$H_s < 1.5$ (%)	$1.5 < H_s < 3$ (%)	$H_s > 3$ (%)	Storm WEF J/m^2
Banyuls	50 m depth	30 mn	Annual	97,678	*0.67*	7.55	*0.49*	5.80	*94.05*	5.65	*0.30*	178,907,104
	42°29.370′ N	6/3/2002	JFM	22,129	*0.84*	4.93	*0.58*	6.19	*89.09*	9.88	*1.03*	
	03°10.060′ E		AMJ	28,675	*0.58*	3.54	*0.40*	5.44	*97.20*	2.78	*0.02*	
			JAS	27,294	*0.46*	2.08	*0.29*	5.04	*99.51*	0.49	*0.00*	
			OND	19,580	*0.89*	7.55	*0.57*	6.86	*87.45*	12.26	*0.30*	
Leucate	40 m depth	30 mn	Annual	104,850	*0.65*	5.57	*0.50*	5.76	*94.88*	4.57	*0.55*	240,422,442
	42°55.000′ N	12/16/2006	JFM	24,608	*0.77*	5.57	*0.57*	6.08	*92.35*	6.49	*1.16*	
	3°07.500′ E		AMJ	25,536	*0.60*	3.67	*0.43*	5.48	*96.46*	3.47	*0.08*	
			JAS	28,229	*0.45*	2.27	*0.27*	5.21	*99.54*	0.46	*0.00*	
			OND	26,477	*0.80*	5.47	*0.58*	6.33	*90.72*	8.25	*1.03*	
Sète	30 m depth	30 mn	Annual	125,546	*0.63*	5.58	*0.53*	6.28	*93.90*	5.16	*0.94*	266,033,640
	43°22.290′ N	5/22/2003	JFM	33,721	*0.76*	5.58	*0.63*	6.61	*91.33*	6.90	*1.77*	
	3°46.777′ E		AMJ	29,368	*0.54*	3.67	*0.39*	6.10	*96.53*	3.36	*0.11*	
			JAS	33,099	*0.42*	3.35	*0.25*	5.44	*98.04*	0.95	*0.02*	
			OND	29,358	*0.82*	4.80	*0.65*	6.87	*88.44*	9.71	*1.85*	
Espiguette	32 m depth	30 mn	Annual	48,917	*0.67*	4.26	*0.50*	5.81	*93.63*	5.95	*0.41*	233,338,937
	47°24.660′ N	8/17/2008	JFM	11,362	*0.77*	4.26	*0.57*	6.22	*91.61*	7.37	*1.02*	
	04°09.750′ E		AMJ	13,797	*0.58*	3.21	*0.40*	5.68	*96.59*	3.36	*0.04*	
			JAS	13,294	*0.50*	2.85	*0.32*	5.24	*98.50*	1.50	*0.00*	
			OND	10,464	*0.90*	3.81	*0.61*	6.20	*85.73*	13.50	*0.76*	

period, the number of major storms is much greater, leading to a standard deviation between 0.57 and 0.65 (Table 1). Wave energy also displays spatial variability, especially during storm events, which are more energetic in the northern part (Sète station). The southern part of the Gulf of Lions is protected from S–SE storms by the rocky Pyrenees coast. Storm waves from the E are shore-normal in the southern part and oblique in the central and northern parts, whereas the most frequent SE storm waves are oblique in the southern part and more or less shore-normal in the central and northern parts. Current patterns essentially depend on the wave energy and are dominated by a longshore component. Current velocities are close to 0.1 $m \cdot s^{-1}$ during fair weather, and can reach 1.0 $m \cdot s^{-1}$ during storms (Certain et al., 2005a; Ferrer et al., 2011; Robin et al., 2014).

3. Methods

3.1. Beach morphology

Beach morphological states and bar types were identified from very high-resolution beach morphological analysis conducted from data obtained from a topo-bathymetric LiDAR survey of the Gulf of Lions coast in summer 2009 (DREAL-LR). To determine modal beach states, the LiDAR analysis also draws on previous studies on bar shapes at regional or local scales that were based on extensive analysis of aerial photographs (Barusseau and Saint-Guily, 1981; Certain, 2002; Michel et al., 2011; Aleman et al., in preparation) and field reconnaissance (Barusseau et al., 1994; Akouango, 1997; Certain, 2002; Certain and Barusseau, 2005; Ferrer et al., 2009; Gervais et al., 2012). LiDAR bathymetry has the advantage of clearly depicting the subaqueous beach morphology and the complex bar patterns, especially in the very low microtidal range setting of the Gulf of Lions (Aleman et al., 2011). The summer 2009 survey was conducted following several weeks of beach stability and with clear waters, enabling the accurate 3D mapping of modal beach states. The LiDAR system consisted of a LADS Mk II, deployed on a Dash 8-202 aircraft flying between 360 and 670 m. The green laser (e.g., bathymetric beam) frequency was 900 Hz, for a minimal spatial resolution of approximately 5 m and for a 240 m-wide swath. The distance between flight lines was 220 m (with a 20 m overlap). Transversal flights over the coastline were also conducted every 5000 m. The data collected extended from the aeolian dune backing the beach to 20 m water depth. The total area covered was 300 km^2 and included 25 million measured points. Airborne LiDAR systems such as LADS MkII are particularly suitable for surveys of large coastal areas such as wide embayments or wide beach corridors (Saye et al., 2005; Shrestha et al., 2005; Montreuil et al., 2014). The LiDAR survey and post-processing data were carried out by EUROSENSE and FUGRO LADS Corporation. Because of the presence of rock outcrops, we carried out a specific control of the accuracy of the LiDAR data on stable subtidal areas. This highlighted vertical and horizontal accuracies of ± 0.30 m and ± 2.98 m, respectively (Aleman, 2013).

A Digital Elevation Model (DEM) was established from the LiDAR data using Fledermaüs IVS7 software based on a "Number of Sample" and "Neighbourhood" algorithm. The beach slope, an additional descriptor of beach state that is complementary to the parameter Ω (see Section 3.4), was determined from 161 beach profiles extracted every kilometre from the LiDAR using ArcGIS 10 Spatial Analyst and 3D Analyst tools. The profiles covered the subaerial beach (excluding urban areas) up to the maximum depth probed by the LiDAR (between −15 and −20 m depth). The DEM and profiles were referenced to tides monitored at two control points in Port-la-Nouvelle and Port Camargue harbours. Tide data from the French Navy (Service Hydrographique et Océanographique de la Marine, SHOM) (Port-Vendres, Sète and Saintes-Maries de la Mer) were also used. Technical support and expertise on tides, as well as data validation, were provided by SHOM (Vanroye, 2009).

3.2. Sediments

In order to determine the sediment fall velocities used in beach state classification on the basis of the parameter Ω, sediment samples were collected every kilometre in the same locations as those of the profiles generated from the LiDAR data. Samples were taken from both the subaerial beach surface (1–2 cm depth) and from the nearshore zone. Nearshore samples were collected with a conical dredge over a depth of 5 cm. Six morphological zones were sampled: (1) the upper beach, (2) the active berm at the landward limit of the swash, (3) the beach step, (4) the crest of the inner bar, (5) the crest of the outer bar when it was present, and (6) the lower shoreface at around −6 to −8 m, which marked the transition to a more regular and gentler slope than that of the bar zone. A total of 805 samples were collected and analysed in the laboratory. Short stretches of rocky coast were excluded from sampling. The sieving method was chosen because most laboratory

grain-size archives have been obtained in this way. The sediment was sifted using an AFNOR column (10, 8, 6.3, 5, 4, 3.15, 2.5, 2, 1.6, 1.25, 1, 0.8, 0.63, 0.5, 0.4, 0.315, 0.25, 0.2, 0.1, 0.08, 0.063, 0.05 mm) with corrected mesh to obtain the median particle size. The average median particle sizes of the subaerial (upper beach, berm and beach step) and subtidal zones (inner bar, outer bar and lower shoreface) were computed. The fall velocity was calculated using the equation of Gibbs et al. (1971).

3.3. Wave parameters

Hydrodynamic data (significant wave height (H_s) and peak period (T_p)) were obtained and analysed by statistical methods from the four stations along the Gulf of Lions coast (Fig. 1B). Offshore-directed waves are associated with offshore winds and are not relevant to the work we present here. Data on waves approaching from 225 to 315° for the southern part and 315 to 45° for the northern part were discarded. Each part of coast was linked to a buoy, the choice guided by coastal morphology and orientation, and by previous wave climate studies in the Gulf of Lions (Guizien, 2009; Gervais, 2012; Aleman, 2013). Finally, offshore wave data were used to characterise breaking conditions. Several expressions for computing breaking wave height (H_b) with different slopes (upper-shoreface, lower shoreface and entire shoreface described in the paragraph 2) were tested by comparison with in situ wave data in the breaker zone (Certain et al., 2005a; Gervais, 2012; Robin et al., 2014). The relationship proposed by Sunamura and Horikawa (1974) yielded the best results when the entire shoreface slope is considered, and was used to compute H_b from the offshore wave conditions:

$$\frac{H_b}{H_0} = (\tan\beta)^{0.2}\left(\frac{H_0}{L_0}\right)^{-0.25}$$

where H_b is the breaker height, H_0 and L_0 are respectively the deepwater wave height and length, and $\tan\beta$ is the gradient of the entire shoreface.

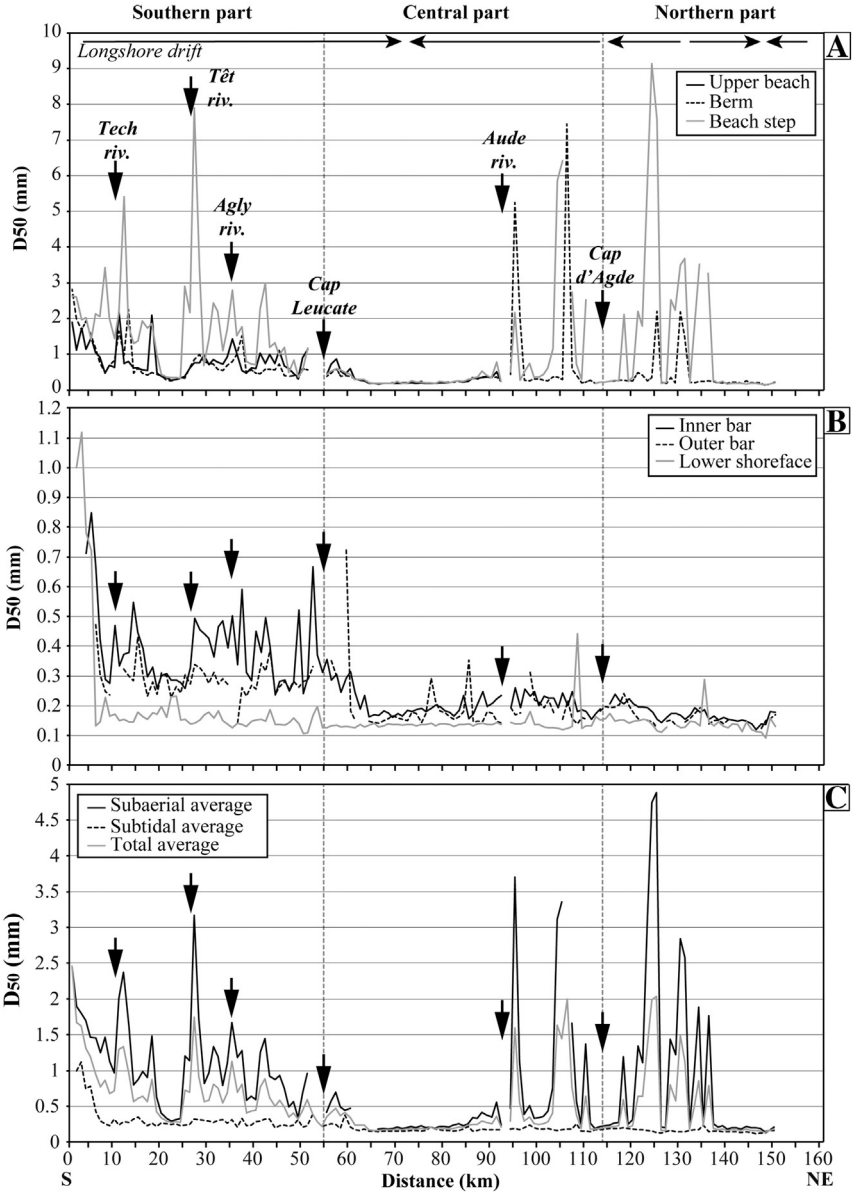

Fig. 3. Longshore distribution of median grain size for 9 sample locations: upper beach, berm, beach step, inner bar, outer bar, lower shoreface, subaerial average, subtidal average and total average.

3.4. The parameter Ω

The parameter Ω was computed to predict the beach morphological state. Wright et al. (1985) showed that beach morphology may be best related to average, rather than instantaneous, wave conditions. Under a low-energy context, such as along the Gulf of Lions, the morphological response is more sensitive to changing wave conditions (Hegge et al., 1996; Jackson et al., 2002; Costas et al., 2005; Gómez-Pujol et al., 2007). As a result, time averages representative of annual, seasonal, monthly and storm wave conditions have been calculated to establish the parameter. In order to ascertain the effects of cross-shore sediment gradation, several sample positions on the beach profile (upper beach, berm, beach step, inner bar, outer bar and lower shoreface) were used. Moreover, using LiDAR data and employing the beach model of Wright and Short (1984), (Aleman et al., 2011) conducted a field classification that recognized the following bar types: (Reflective (R), Longshore Bar-Trough (LBT), Rhythmic Bar and Beach (RBB), Transverse Bar and Rip (TBR), Low Tide Terrace (LTT) and Dissipative (D)). The hierarchical classification framework proposed by Loureiro et al. (2013) was then used to obtain field values of Ω for all profiles surveyed every kilometre. Assessment of Ω was then based on comparison of the field classification with predicted beach states.

4. Results

4.1. Sediments

The superficial sediment of the aerial beach and the shoreface consists of well-sorted sand according to Folk and Ward (1957). Regionally, the sediments become gradually finer-grained northward. This implies a difference between the southern part (medium-coarse sands, 0.25–1.60 mm), where the influence of river sand supply is appreciable, and the central and northern parts located updrift of river mouths (fine-medium sands 0.17 mm) (Fig. 3). The boundary between these two parts is represented by Cape Leucate (Fig. 3), which corresponds to a semi-impermeable barrier to longshore sediment transport (Brunel et al., 2014). Longshore variations can be also observed on a smaller scale, for example in the vicinity of river mouths or in front of nearshore rock flats. The sediment of the beach step shows greater heterogeneity than that of other units of the system, such as the berm and nearshore zone (Fig. 3).

Cross-shore variations are observed with an overall seaward decrease in grain size. This variation is greater in the southern and northern parts of the study area where the standard deviation between each box of the system is higher (Fig. 4). In contrast, the lower shoreface is very homogeneous on a regional scale (Fig. 3). On the adjacent shelf, sediment is mostly composed of sand down to 25–30 m water depth, and muddy silts between 25 and 40 m depth (Aloïsi et al., 1973).

4.2. Beach states

Six beach states were identified (Fig. 5) based on bar types, profile shape (Fig. 6), sediment characteristics and local specificities of the shoreface. Several beach state sectors were thus identified along the 200 km of coastline (Fig. 7). Specific attention was paid to the inter-class transitions (Fig. 8).

4.2.1. Reflective beaches

Reflective beaches are characterised by an abrupt profile and the absence of nearshore bars (Aleman et al., 2011) (Figs. 5, 6). This beach state (5 profiles, 1.1% of the coastline, Fig. 7) is only observed in a confined cell in the southern part of the study area between the rocky Pyrenees coast and harbour jetties to the north (Fig. 8A). The sediment is coarse on the subaerial beach (D_{50} = 1.86 mm) and medium in the subtidal zone (D_{50} = 0.91 mm) (Fig. 5). The slope is steep and attains an average of 1.16° (Fig. 5).

4.2.2. Intermediate beaches

An intermediate beach state occurs only in the southern part (47 profiles, 23.6% of the coastline) (Fig. 7). The southern boundary with the reflective beach zone is represented by the harbour jetties mentioned above (Fig. 8A). To the north, this beach state is limited by Cape Leucate (Fig. 8B). Intermediate beaches exhibit well-developed RBB to TBR morphology. Usually two bars are present but an additional bar close to the beach is also sometimes observed. This bar displays complex features with a long platform that extends along the beach, and small transverse bars that can occasionally be connected with the inner bar (Aleman et al., 2011) (Fig. 5). The median grain size is coarse in the subaerial zone (D_{50} = 1.03 mm) and fine in the subtidal zone (D_{50} = 0.27 mm) (Fig. 5). The slope of the beach is 0.87° on average (Figs. 5, 6).

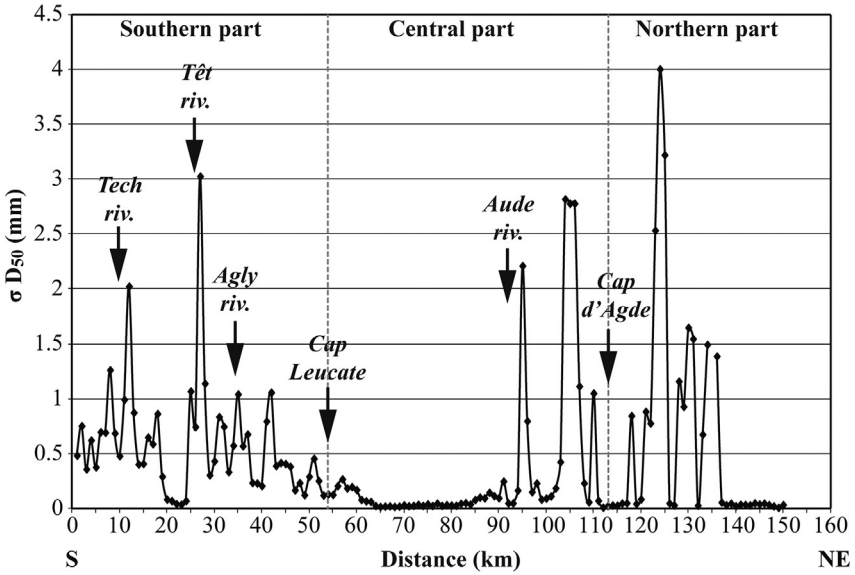

Fig. 4. Longshore evolution of the D_{50} standard deviation for the 6 sediment sample location sites (upper beach, berm, beach step, inner bar, outer bar and lower shoreface).

4.2.3. Intermediate–dissipative beaches

Intermediate–dissipative beaches are observed at the western end of the northern part (11 profiles, 10.3% of the coastline, Fig. 7) between Capes Agde and Mont Saint Clair (Fig. 8C, D), as well as along Espiguette spit (11 profiles, 6.9% of the coastline), where the boundary consists of harbour jetties (Fig. 8F). This beach state is characterised by an inner RBB and an outer LBT that grades to D (Aleman et al., 2011) (Fig. 5). The sediment is composed of fine sand in the subtidal zone (D_{50} = 0.18 mm) and medium sand in the subaerial zone (D_{50} = 1.10 mm) (Fig. 5) and the slope is lower with an average of 0.5° (Figs. 5, 6).

4.2.4. Dissipative beaches

Dissipative beaches are found between Capes Leucate (Fig. 8B) and Agde (Fig. 8C). They exhibit two straight bars in a transition from LBT to D. Another small bar can be observed close to the shore (Aleman et al., 2011) (Fig. 5). The beach profile differs from the previous one

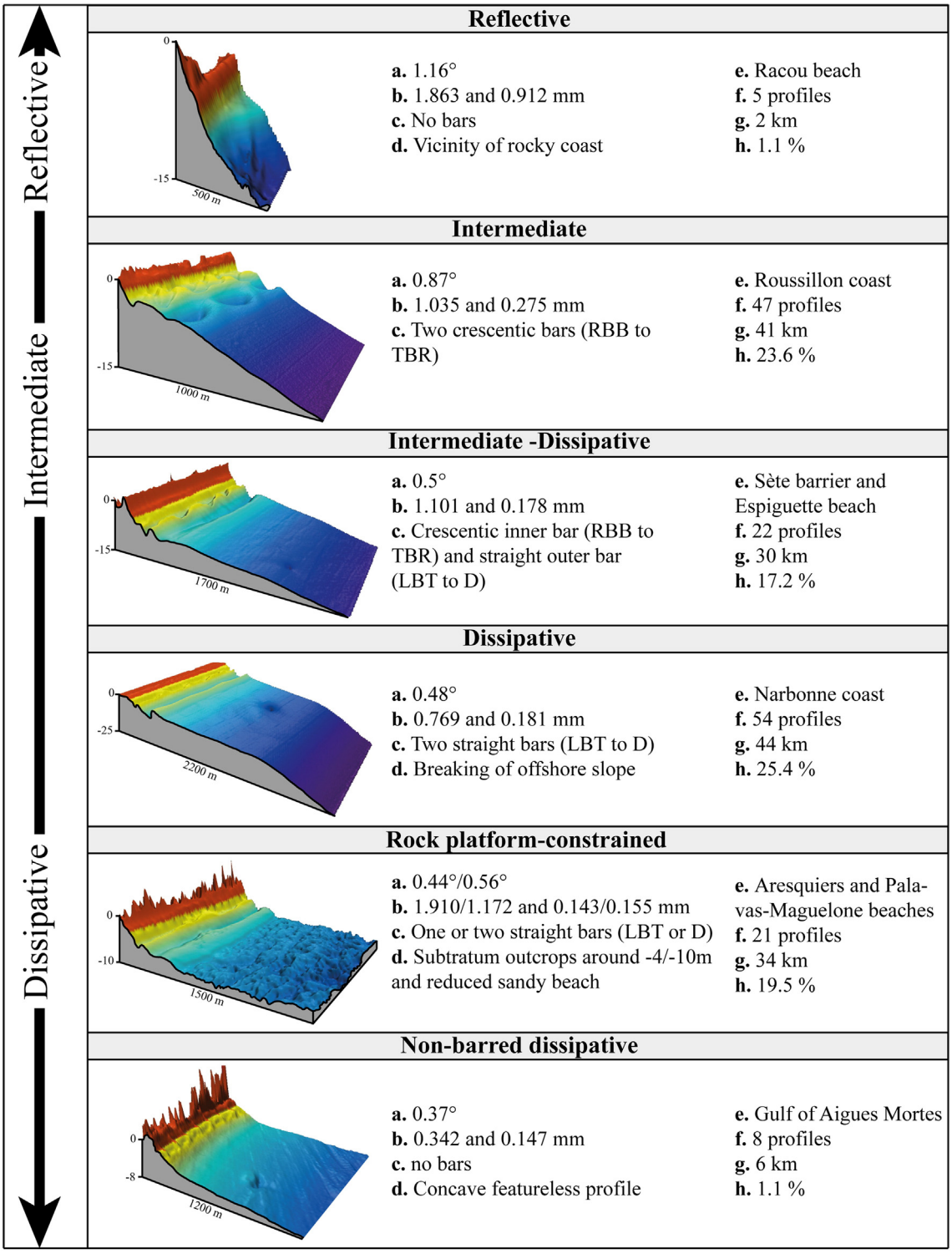

Fig. 5. 3D classification of beaches observed in the Gulf of Lions. (a) Shoreface slope, (b) median particle size of sediment from subaerial and subtidal areas, (c) number of bars, (d) profile shape, (e) location of beach state compartment, (f) number of profiles, (g) kilometres of coast and (h) percentage of coast.

by a break in slope at −15 m, evolving into a convex configuration offshore (Figs. 5, 6). Subtidal sand is fine with a D_{50} of 0.18 mm, whereas supratidal sand is medium (D_{50} = 0.77 mm) (Fig. 5). The average slope is 0.48° (1.03° for the steepest offshore profile). These states prevail only in the central part (54 profiles, 25.4% of the coastline, Fig. 7).

4.2.5. Rock platform-constrained beaches

Beaches constrained by a rock platform are a sediment-poor beach type marked by the presence of a substratum composed of bedrock outcrops on the shoreface. For the Aresquiers area (7 profiles, 5.7% of the coastline, Fig. 1), the substratum appears between −3 and −5 m overlain by a very thin sand sheet forming the beach. These beaches exhibit one or two straight bars with a slightly more marked outer bar. The grain size consists of subaerial coarse sand (D_{50} = 1.91 mm) and subtidal fine sand (D_{50} = 0.14 mm) (Fig. 5). The slope of the sand system is 0.44° (Fig. 5). In the Palavas-Maguelone area (14 profiles, 13.8% of the coastline, Fig. 1), the substratum appears at a depth of −10 m (Figs. 5, 6). The sand sheet is thus thicker than in the previous zone. The subaerial grain size is slightly finer (D_{50} = 1.17 mm) (Fig. 5) and the beach gradient larger (0.56°) than in the Aresquiers area (Figs. 5, 6). The two areas of beach constrained by a rock platform are contiguous and the transition occurs progressively over 2 km. The southern boundary corresponds to Mont Saint Clair (Fig. 8D), whereas the northern boundary with the non-barred dissipative beaches is gradual over a few kilometres, despite the presence of several coastal engineering structures (Fig. 8E).

4.2.6. Non-barred dissipative beaches

Non-barred dissipative beaches are only observed in the inner part of Aigues Mortes Bay (4 profiles, 0.6% of the coastline, Fig. 7). The southern boundary is gradual (Fig. 8E) whereas the northern limit with the intermediate–dissipative beaches corresponds to the jetty on Espiguette spit (Fig. 8F). These beaches exhibit a characteristic concave profile, with the gentlest slope (0.37°) (Figs. 5, 6) and the finest grain size

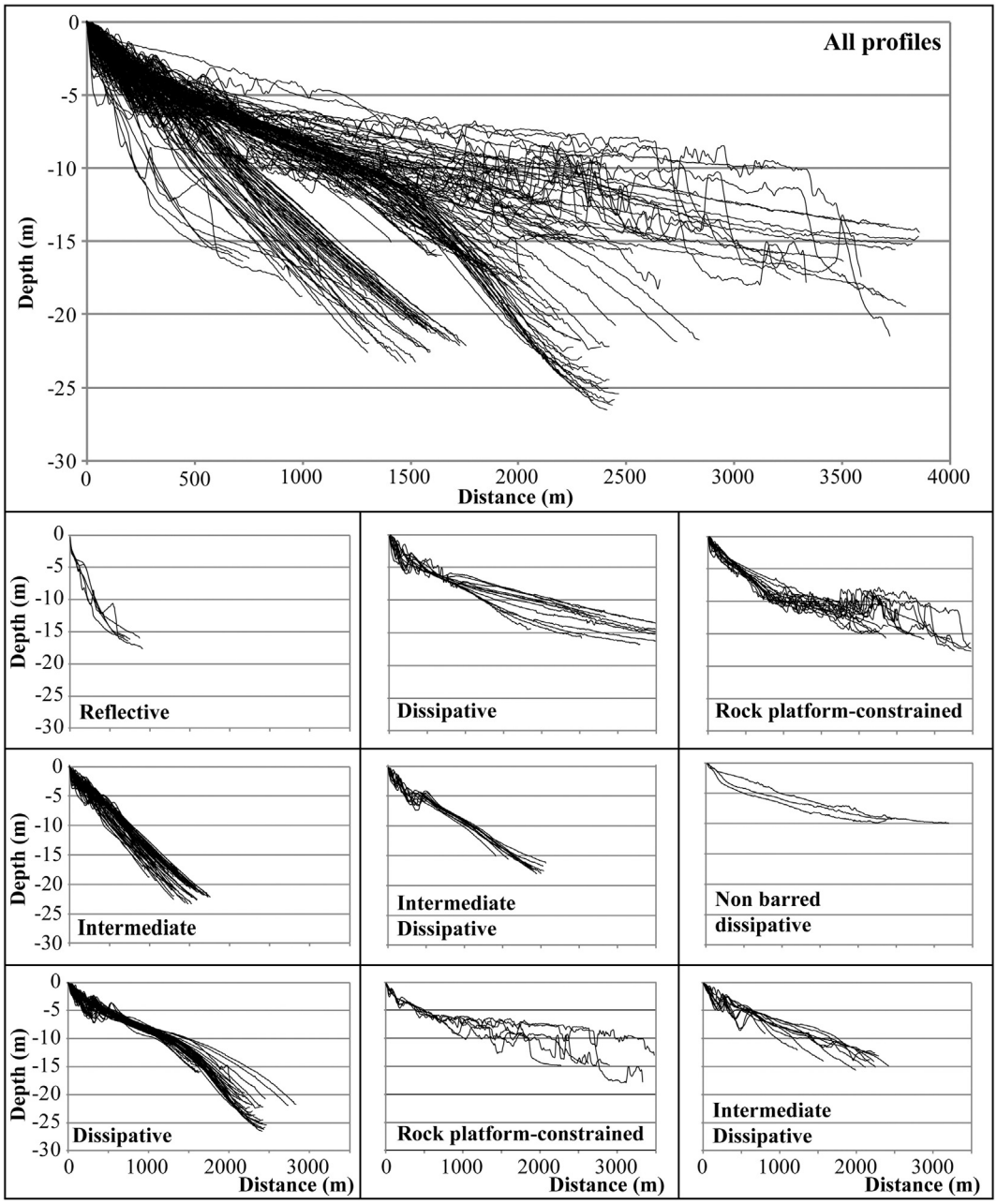

Fig. 6. All beach profiles extracted from LiDAR data and selected profiles representing the different morphological compartments (see Fig. 7 for location).

(0.34 mm (subaerial area) and 0.15 mm (subtidal area)) throughout the study area (Fig. 5). This state does not usually display bars, but a single bar is occasionally observed (Figs. 5, 6).

4.2.7. Spatial transitions and extension of beach class compartments

The longshore transition between each beach class compartment is generally abrupt and limits are often formed by rock headlands (Figs. 8B, C, D, F, and Table 2). Only at the reflective-intermediate transition does a harbour constitute the boundary (Fig. 8A). However, this transition was already apparent on aerial photographs taken before the construction of the harbour (Fig. 9). In no other situation do harbours and coastal defences exhibit a relationship with beach class distribution (Figs. 8G, H). Beach state compartments extend from a few kilometres to several tens of kilometres (Fig. 7). Transitions are marked by a change in slope and sediment size, except between intermediate–dissipative and dissipative compartments (Table 2). The number of occurrences and percentages of the occurrence of each observed beach state are shown in Fig. 5. In the Gulf of Lions, the most frequent beach state is the dissipative state (25.9%), followed by the intermediate, the rock platform-constrained and intermediate–dissipative states, with respectively 23.6%, 19.5% and 17.2% of occurrence.

4.2.8. Modal beach states

Comparison of the results of this study with previous research emphasizes that beach states are spatially persistent at the multi-decadal scale. Only the bar types may evolve from one stage to another over the short term in response to seasonal variability in wave conditions. Fig. 10 shows three aerial photographs taken in 1968, 1986 and 2009, depicting the intermediate and dissipative compartment. Thanks to the transparency of the water, these pictures show beach states that have remained the same over the 41-year period. Thus, the 2009 LiDAR provides a reliable larger-spatial scale overview of the modal beach states.

4.3. Observed versus predicted beach states

Beach states in the study area were predicted using the parameter Ω based on various combinations of wave statistics (mean annual, mean spring/summer/autumn/winter, storm, August 2009) and grain settling velocities (upper beach, berm, beach step, inner bar, outer bar, lower shoreface, overall mean, subaerial mean, subtidal mean) for all LiDAR profiles (every kilometre). Fig. 11 shows, for instance, the mean Ω values obtained for combinations of wave climate and settling velocities for the six beach state compartments. The grey background indicates the bar types observed on the LiDAR bathymetry (Aleman et al., 2011) and converted to Ω values according to the Wright and Short (1984) model using the hierarchical classification proposed by Loureiro et al. (2013). The results show a large spread of Ω. The best predictions are those derived from the use of subtidal grain size while storm conditions yield poor results.

The ratios between observed values of the parameter Ω (Ω_o) and predicted values (Ω_p) for the various beach states (Reflective, Intermediate and Dissipative) are shown in Table 3. The use of upper beach, berm, beach step, lower shoreface and subaerial settling velocities yields poor Ω_o/Ω_p correlations (<50%), except for the berm with storm conditions (60.7%). Better ratios are associated with inner or outer bar crest settling velocities (between 63.1 and 77.0%), with the subtidal mean (72.3 to 84.5%) and with the overall mean (51.3 to 60.7%). A best ratio (84.5%) is obtained using the subtidal mean settling velocity with mean wave conditions over a period of one month prior to the observed beach states (August 2009, Table 3). Storm conditions yield low ratios except with berm settling velocities (60.7%, Table 3).

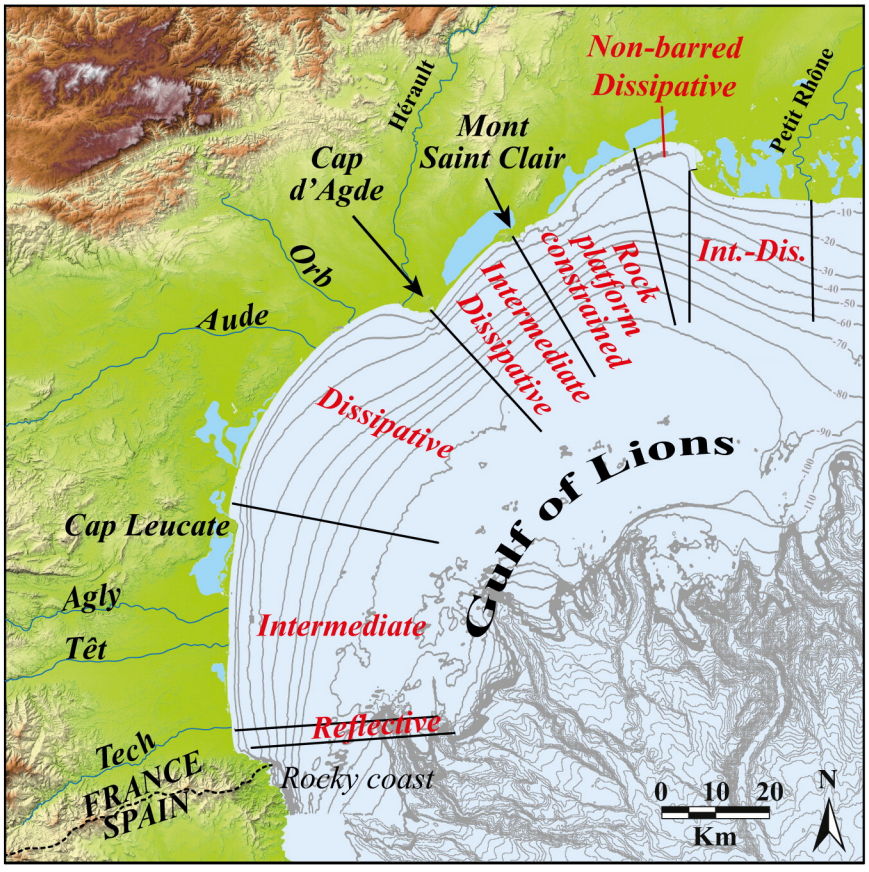

Fig. 7. Location of morphological compartments identified on the Gulf of Lions coast.

Ratios of Ω_o/Ω_p for bar types as defined by Aleman et al. (2011) are shown in Table 4. Ω_o/Ω_p correlations for bar types are weaker than for beach states. Ω_p values computed with settling velocities on the upper beach, berm, beach step and lower shoreface are poorly related to Ω_o (x` 4). Better correlations are obtained with settling velocities from the inner or outer bars, especially for autumn and winter waves (60.3 to 64.8%). The best Ω predictions, with a ratio of 72.3%, are obtained using the mean settling velocity of the subtidal zone and the mean annual wave conditions prior to the observation of bar types. As in the case of beach states, storm conditions yield poor results (<50%), whatever the sediment fall velocity used.

Fig. 12 shows the spatial variability of Ω for combinations of settling velocities and wave conditions that yield the best correlations with the observed morphologies. The observed bar types are represented by a grey background. The results show large fluctuations in Ω_p over short distances, especially in the intermediate and dissipative domains. The general trend is consistent with the observed bar types, with a progressive upstate shift from the reflective to the dissipative domain (Fig. 12). However, for inner bar sediments, Ω_p tends to underestimate the observed morphologies in the intermediate area. The best predictions are obtained for the reflective and dissipative fields (Fig. 12). For outer bar sediments, better predictions are obtained for the intermediate domain, but the bar types of the intermediate–dissipative domain are over-estimated (Fig. 12). Finally, the best predictions are obtained when the mean subtidal sediment fall velocities are combined with annual or August 2009 wave conditions. In this case, the majority of differences between Ω_o/Ω_p are located in the intermediate field with a slight under-estimation of the observed morphologies (Fig. 12).

5. Discussion

The discussion will focus on the following selected themes that bear on the identification and characterisation of beach states and their transitions, on environmental factors influencing beach states and their distribution, and finally on the validity, skill and limitations of the parameter Ω in characterising and these predicting beach states, based on the exhaustive analysis of combined LiDAR bathymetry data, grain settling velocities and wave data.

5.1. Beach state classification and state transitions

Wright and Short (1984) developed a single-bar beach model for wave-dominated coasts from Australian beaches with six beach states. This model was complemented by Short and Aagaard (1993) who extended it to two- to three-bar systems. Previous studies on Gulf of Lions beaches have enabled the description of complex bar types and

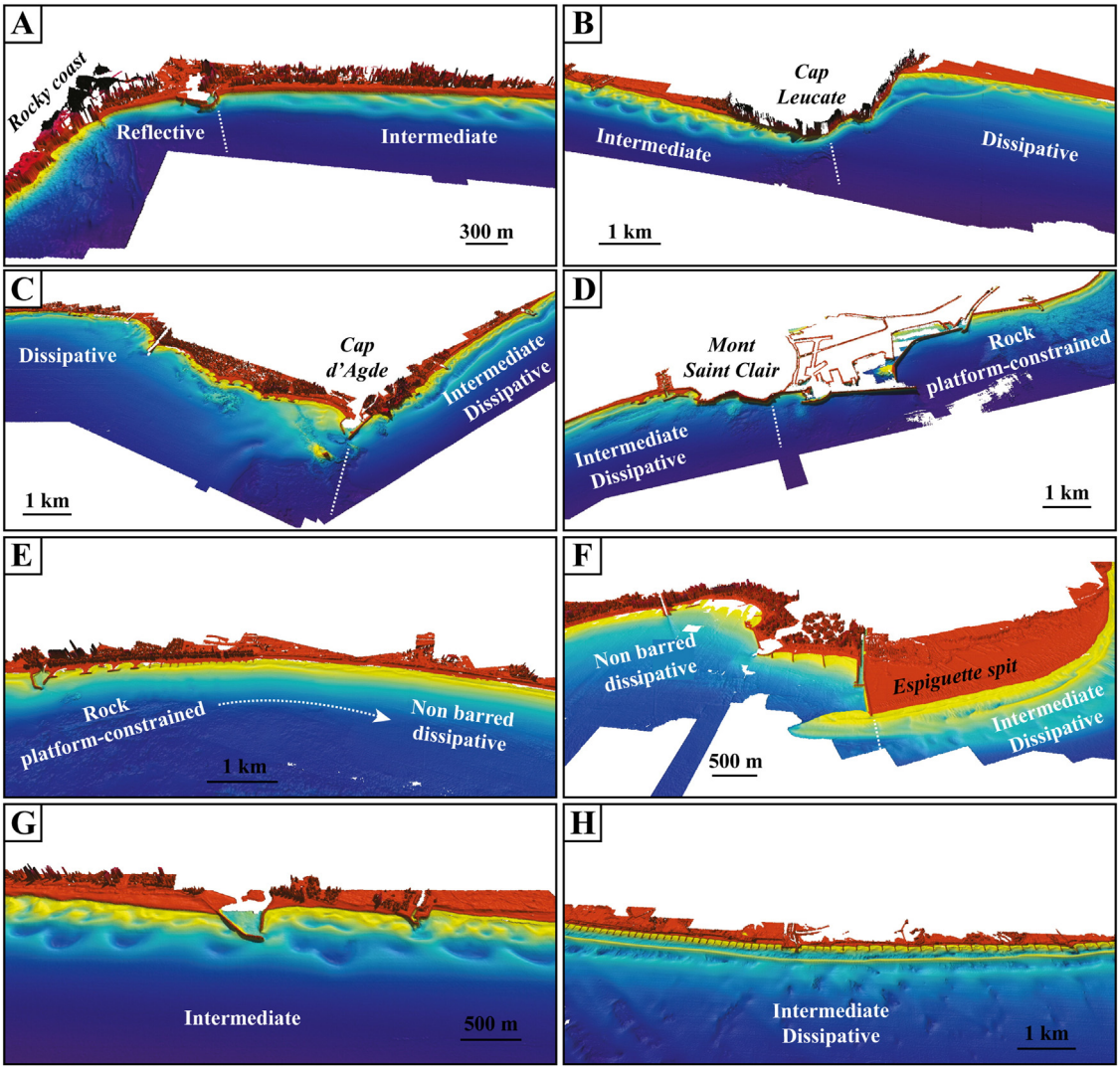

Fig. 8. LiDAR bathymetry of beach state transitions: (A) reflective to intermediate, (B) intermediate to dissipative, (C) dissipative to intermediate–dissipative, (D) dissipative to rock platform-constrained, (E) rock platform-constrained to non-barred dissipative, and (F) non-barred dissipative to intermediate–dissipative. The last two images show beach states uninfluenced by (G) harbours or (H) coastal defences.

Table 2
Characteristics of the boundaries and variations in sediment particle size and slope between each morphological compartment.

Transition	Boundaries	Particle size	Slope
Reflective to intermediate	Harbour/progressive	Decreases	Decreases
Intermediate to intermediate–dissipative	Cape	Decreases	Decreases
Intermediate–dissipative to dissipative	Cape	Constant	Constant
Dissipative to rock platform-constrained	Cape	Increases	Increases
Rock platform-constrained to non-barred dissipative	Progressive	Decreases	Decreases
Non-barred dissipative to dissipative	Harbour	Increases	Increases

transitions over short distances (Ferrer et al., 2009; Aleman et al., 2011), the latter study based on high-resolution 3D LiDAR data. Using a combination of aerial photograph data and such 3D data, the present study shows, on a regional scale, a large diversity of beach states with several morphologically continuous states over several kilometres. Although the bars exhibit complex morphology and 3D patterns, they are classic systems with respect to the literature, both from a morphological (this study) and a dynamic point of view (Aleman et al., 2013).

The associated beach states show, however, two unusual or atypical types. First, the rock platform-constrained state (which represents a significant 19.5% of the coastline) presents a steep beachface fronting bedrock that can nourish the berm with pebbles and cobbles. This state is typical of sediment-starved settings with a thin and narrow sand sheet overlying the bedrock. Despite this, one or two straight bars are present in the confined nearshore sandy zone. These bars are small and migrate offshore at a very slow rate (19 $m \cdot year^{-1}$) (Aleman et al., 2013). The rock platform is wide and shallow (−10 m) and bedrock attenuation of stronger waves offshore could explain this relatively slow migration (e.g., Anfuso et al., 2003; Sabatier et al., 2004). Beaches with bedrock/rock flats/reef are common in the literature (Sanderson and Eliot, 1999; Short, 2006), but the presence of bars has, to our knowledge, never been documented. This relatively common beach state on the Gulf of Lions coast is morphologically original, as is the control exerted by bedrock on bars and beachface characteristics. Secondly, despite the fact that the non-barred dissipative state is represented in only a short part of the coast (6 km or about 3% of the studied coast), this state is unusual in a microtidal environment. This concave featureless profile has been mainly identified in meso- and macro-tidal environments (e.g., Short, 2006; Scott et al., 2011). However, it can also occur in sheltered, microtidal, low wave-energy settings characterised by fine sand (Klein et al., 2010), as observed in Aigues Mortes Bay in the northern part of the study area. As reported by Hegge et al. (1996), sediment size apparently determines the morphodynamic state of the beach under sheltered low-energy conditions where the wave fetch is restricted.

Alongshore transitions between bar-beach states, as mentioned in the Introduction, have been rather poorly documented. The use of 3D topo-bathymetric LiDAR in the present study over a regional and almost continuous sandy beach that is nearly 200 km long allows us to bring out these transitions, regarding which this study has highlighted a

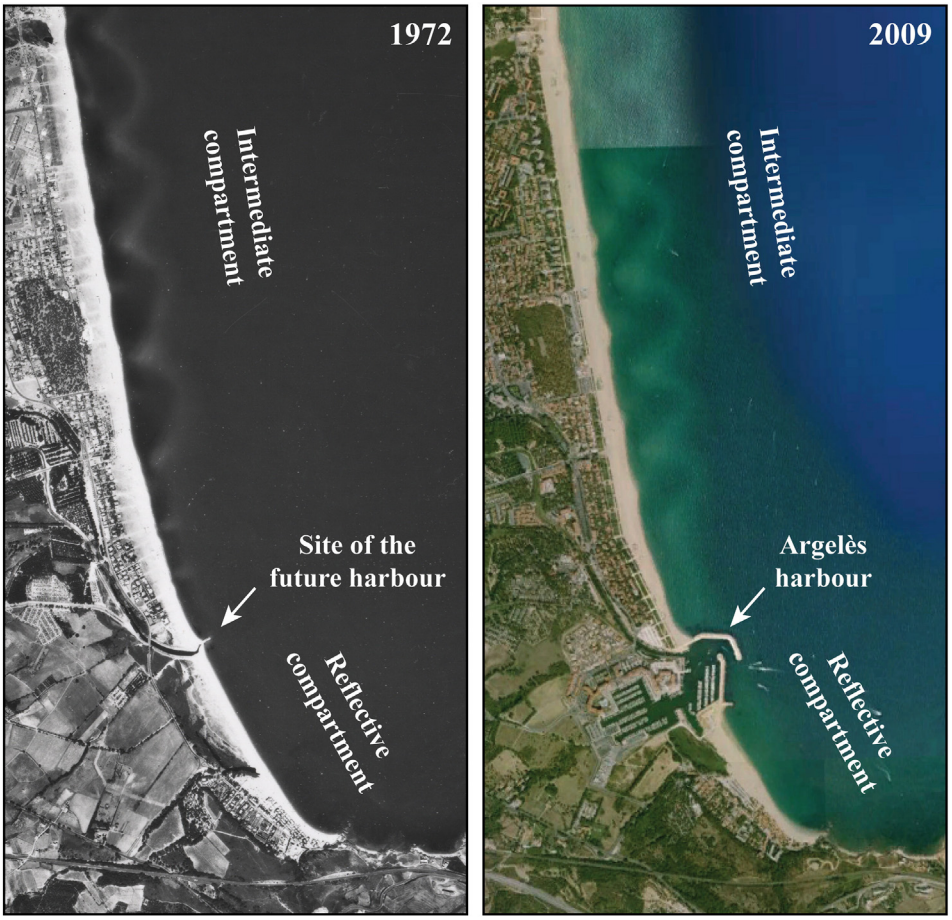

Fig. 9. 1972 and 2009 aerial photographs (©IGN) of the reflective to intermediate transition showing the existence of the transition prior to the construction of Argelès harbour.

number of characteristics: (1) the spatial extent of beach class cells varies from a few kilometres to several tens of kilometres; (2) some transitions are sudden when the beaches are interrupted by large rocky headlands (Cap Leucate, Cap d'Agde, Mont Saint Clair); (3) transitions can also occur progressively over a few hundred metres on continuous beaches, and in these cases, bar patterns are complex and entangled (Aleman et al., 2011); (4) harbours and river mouths do not seem to disturb the regional beach state pattern. Transitions are thus essentially under the overarching influence of geology.

5.2. The influence of the geological framework

Beach state models do not take into account the influence of geological constraints such as headlands, rock outcrops and reefs on the morphodynamics that underlie such classifications. However, several recent studies have emphasized the importance of these constraints, some of which can have an overarching influence on observed beach morphologies (e.g., Jackson et al., 2005; Short, 2006; Jackson and Cooper, 2009; Scott et al., 2011; Loureiro et al., 2013).

First, the presence of capes plays a role in sediment cell size and transport (Sanderson and Eliot, 1999), rip formation (Short, 1999, 2006, 2010), and wave propagation (Gómez-Pujol et al., 2007). It is shown in this study that headlands/capes along the Gulf of Lions coast strongly influence beach and shoreface characteristics. The most clearly expressed influence is observed at Cape Leucate, which forms the boundary between intermediate (southward) and dissipative (northward) beach states, notably through its influence on grain size on either side of the cape. The Cape interrupts medium-coarse sand from the

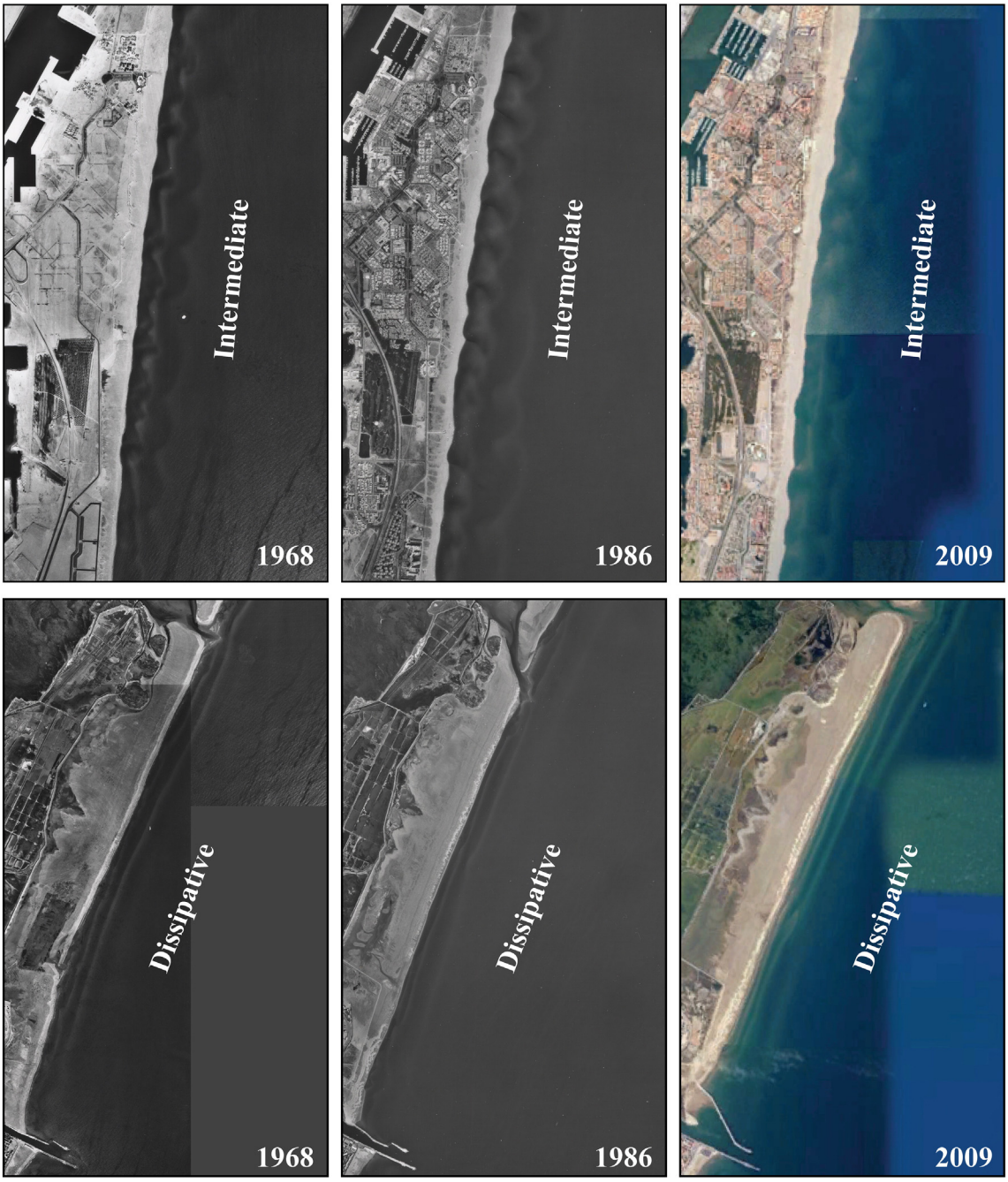

Fig. 10. Aerial photographs (©IGN) taken in 1968, 1986 and 2009 in the intermediate and dissipative compartment. Thanks to the transparency of the water, these pictures show that beach states have remained the same over the 41 years spanned by the photographs.

coastal rivers transported northward by longshore drift, favouring larger fall velocities and intermediate beach states. Fine sand has been shown to be trapped beyond the wave closure depth at about −6 to −8 m (Brunel et al., 2014). However, only a small fraction of this fine sediment can pass through the outer bar and supply the intermediate beaches. Sand transported north of the Cape mostly comes from ancient abandoned lobes of the Rhône delta, located further north, outside the study area, and consists of fine to medium sand associated with dissipative beaches. Another example on the Gulf of Lions coast is that of the rock outcrops north of Mont Saint Clair headland, characterised by the rock platform-constrained beach state (Fig. 5). The influence of Cape d'Agde is more complex but it clearly forms a boundary between dissipative (southward) and intermediate–dissipative (northward) beach states.

Secondly, accommodation space, largely controlled also by the geological context, can have a significant impact on shoreface morphodynamics and observed beach states, as shown in this study and in the literature. Bedrock outcrops not only generate wave energy dissipation (Sanderson and Eliot, 1999; Short, 2006, 2010; Short and Woodroffe, 2009; Muñoz-Perez and Medina, 2010), the emergence of topographic rips (Short, 1999, 2006, 2010), but also influence and constrain sediment accommodation space and the sediment stock (Jackson et al., 2005; Scott et al., 2007, 2011; Jackson and Cooper, 2009). In the northern area, in the rock platform-constrained beach compartment, where the depth of closure is between −6 and −10 m (Sabatier et al., 2004), the substratum crops out at a depth of −5 to −10 m, sediment supply is limited (Certain et al., 2005b), full seaward development of the profile is not possible, and the profile characteristics are modified. Moreover, the bedrock modulates wave energy and limits the onshore transfer of sand between the upper and lower shorefaces. Sediment transfers are observed only during high-energy events, but the input consists of coarse sand or pebbles. This geological context favours shorter and steeper beaches.

5.3. The influence of multi-decadal sediment budget changes on beach states: a tentative approach

Net long-term beach and nearshore sediment budget changes, such as those that have been reported in the Gulf of Lions, may presumably affect long-term beach states and their distributions. If we address the specific problem of multi-decadal sediment budget changes, the shoreface sediment deficit in the western Gulf of Lions over the last 25 years (Brunel et al., 2014) has, apparently, not affected the spatial and temporal persistence of beach states identified in this study. This theme certainly offers scope, however, for further study as climate change and increasing anthropogenic pressures are likely to exacerbate the beach and shoreface sediment budget in the Gulf of Lions in the

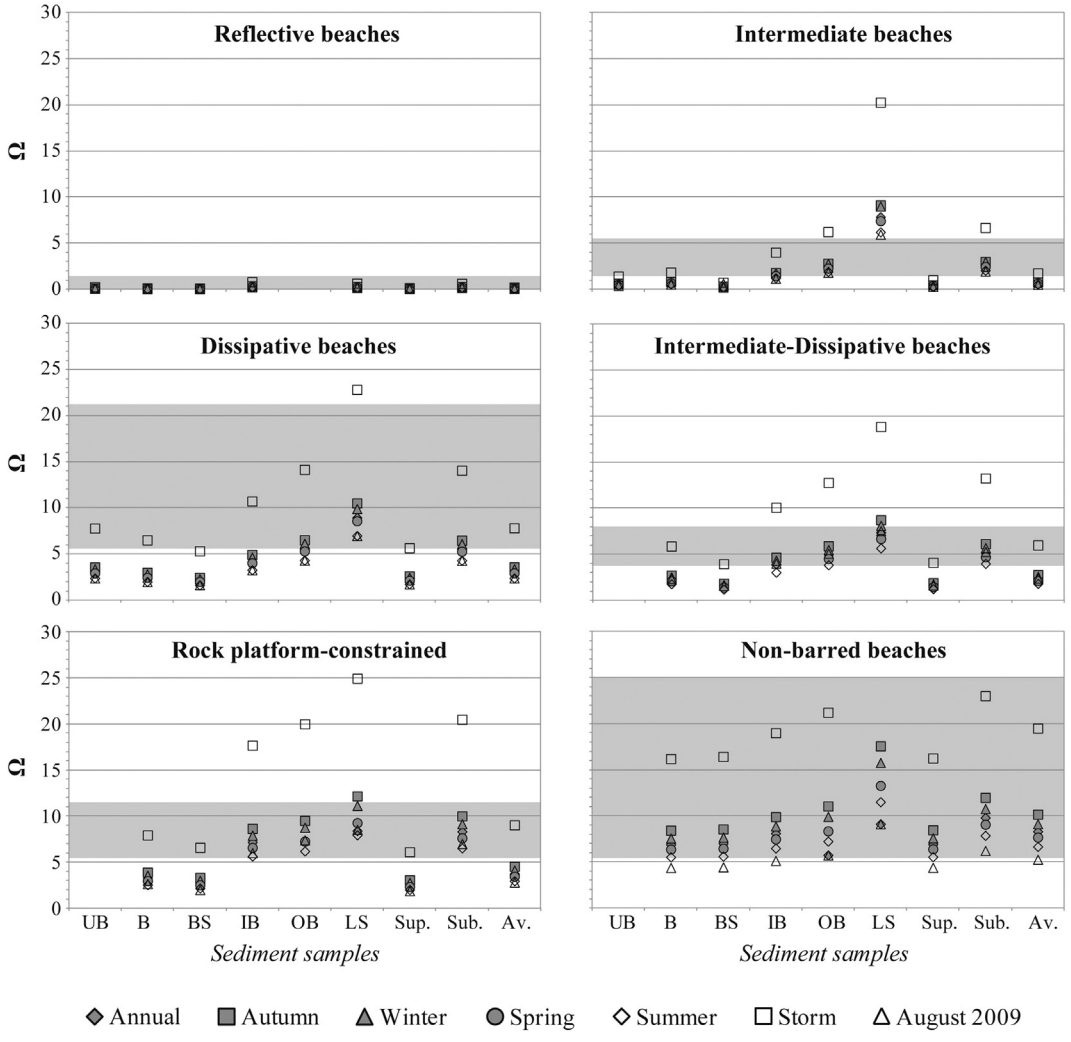

Fig. 11. Cross-shore variation of mean Ω values calculated for wave conditions associated with various seasons or events for the six beach state compartments. Greyscale area corresponds to observed beach state. UB: upper beach, B: berm, BS: beach step, IB: inner bar, OB: outer bar, LS: lower shoreface, Sup.: supratidal average, Sub.: subtidal average, and Av.: all environment average.

Table 3
Percentage of beach state ratios of Ωpredicted/Ωobserved (reflective, intermediate, and dissipative) for all sediment sample locations and hydrodynamic periods.

		Hydrodynamic conditions							
		Annual	Winter	Spring	Summer	Autumn	August 2009	Storm (Hs > 2m)	N sample
Sediment samples	Upper beach	47.7	47.7	46.6	43.2	47.7	42.0	44.3	88
	Berm	44.8	47.6	44.1	37.2	49.7	36.6	60.7	145
	Beach step	33.6	39.2	32.9	30.1	38.5	28.7	41.3	143
	Inner bar	73.3	75.3	71.9	67.1	74.0	65.1	58.2	146
	Outer bar	64.8	67.2	71.3	76.2	63.1	77.0	45.1	122
	Lower shoreface	31.8	31.1	37.2	37.8	30.4	43.2	27.0	148
	Supra. av.	34.7	35.4	34.0	31.3	37.5	30.6	42.4	144
	Sub. av.	77.0	72.3	77.0	83.8	70.3	84.5	43.9	148
	Total av.	60.7	60.7	58.7	51.3	58.7	52.7	56.0	150

%
<10
10–25
25–50
50–60
>60

coming decades, paving the way for disequilibrium in the currently prevailing beach state patterns and their longshore distributions.

It is interesting to note that the theme of the effect of net and persistent sediment budget changes on beach states was tentatively and conceptually approached by Wright et al. (1985) using a long-term form of disequilibrium index based on the parameter Ω, which is further discussed in Section 5.5. This disequilibrium index approach regarding long-term beach state morphodynamic switches liable to be caused by multi-decadal sediment budget variations has, in fact, hardly been further explored in the literature. In a nutshell and following Wright et al. (1985), long-term beach state changes can be induced by environmental parameters acting on H_b that engender disequilibrium by rendering the system more dissipative or more reflective. Among these long-term parameters are sea-level rise, net sediment budget changes or net changes in wave climate such as increased storminess, environmental conditions that are currently causes for concern as far as beach stability goes.

5.4. The influence of coastal engineering structures

Regarding harbours in this study, only one of twelve constitutes a boundary between the reflective and intermediate states. However, the aerial photographs prior to, and following harbour construction suggest that this transition has always been in existence and is not directly related to the vicinity of the harbour (Fig. 9). The 3D subaqueous LiDAR data suggest that harbour breakwaters have very local impacts on bar morphology where such bars are intersected by jetties, and generate only slight changes in the subaqueous slope. Smaller coastal structures such as groynes do not seem to affect the regional/local beach state. Their impact is generally limited to highly localized rips and complex bar patterns in shallow water (Aleman et al., 2011). The impact of engineering structures in the microtidal Mediterranean setting of the Gulf of Lions appears to be much lower than that of the modally high-energy, storm-dominated coast of the Netherlands (Short, 1992).

5.5. The Ω parameter

Important discrepancies have been observed between the predicted and observed beach morphologies using the Ω as a descriptor of beach states (Wright et al., 1987; Sanderson and Eliot, 1999; Benaventes et al., 2000; Klein and Menezes, 2001; Thieler et al., 2001; Jackson et al., 2005; Loureiro et al., 2013). However, in these cited examples the authors concluded on the usefulness of this parameter in discriminating between the extreme reflective and dissipative beach states,

Table 4
Percentages of bar type ratios of Ωpredicted/Ωobserved (R, LTT, TBR, RBB and D) for all sediment sample locations and hydrodynamic periods.

		Hydrodynamic conditions							
		Annual	Winter	Spring	Summer	Autumn	August 2009	Storm (Hs > 2m)	N sample
Sediment samples	Upper beach	13.6	20.5	5.7	3.4	26.1	3.4	11.4	88
	Berm	5.5	11.0	4.8	1.4	15.9	2.1	36.6	145
	Beach step	9.8	16.1	7.0	2.1	16.8	0.7	24.5	143
	Inner bar	52.1	52.1	41.1	21.2	60.3	22.6	39.0	146
	Outer bar	53.3	64.8	54.9	43.4	60.7	42.6	36.9	122
	Lower shoreface	29.7	28.4	31.8	39.9	31.1	41.9	2.7	148
	Supra. av.	6.9	9.7	4.2	2.1	16.0	1.4	23.6	144
	Sub. av.	72.3	69.6	66.2	62.8	66.9	67.6	37.8	148
	Total av.	24.7	30.7	22.0	10.0	31.3	8.7	29.3	150

%
<10
10–25
25–50
50–60
>60

but on its inadequacy in characterising intermediate states (Wright et al., 1987; Bauer and Greenwood, 1988; Ranasinghe et al., 2004; Grasso et al., 2009; Scott et al., 2011; Loureiro et al., 2013).

Marked variability can occur in calculated Ω values depending on the sediment sample location across the active profile, as shown by Benedet et al. (2004a). The poor Ω_o/Ω_p correlations with subaerial settling velocities in a microtidal context may be due, for instance, to the infrequent inundation of the upper beach which is affected by surge that can cause pronounced differences in sediment characteristics between the subaerial and subtidal beach, as reported by Jackson et al. (2002). Subtidal environments such as the inner bar, outer bar and lower shoreface tend to yield more realistic values. Gómez-Pujol et al. (2007) noticed that the parameter Ω could be useful in gross beach classification but tends to fail with seasonal variability. Jiménez et al. (2008) emphasized the importance of taking into account the duration and intensity of the wave forcing necessary for the morphological reaction of

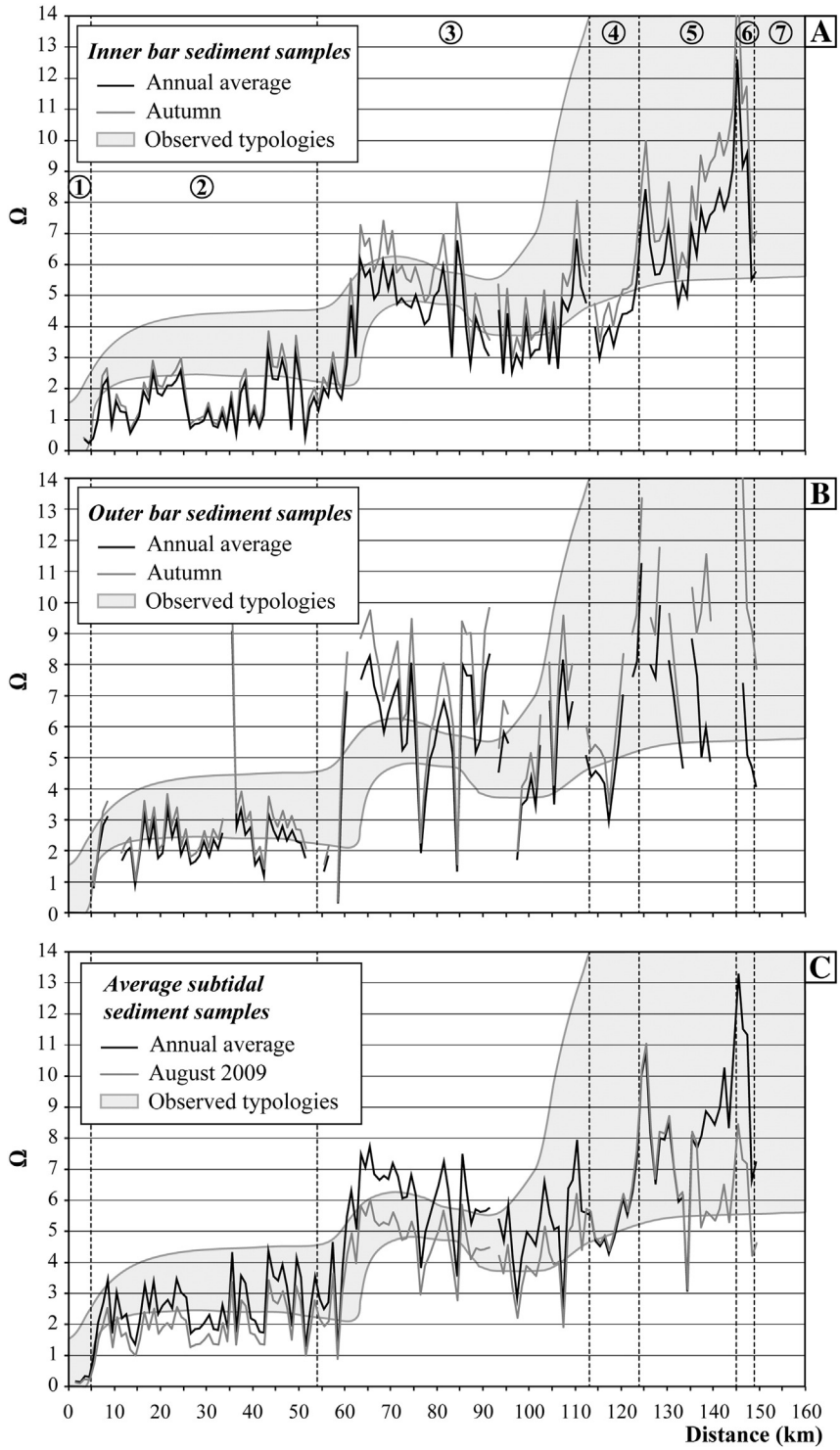

Fig. 12. Longshore variation of the Ω parameter that yields the best correlations with the observed morphologies: (A) inner and (B) outer bar sediment samples with annual and autumn wave conditions, and (C) average subtidal sediment samples with annual and August 2009 wave conditions. The circled numbers indicate the morphological compartments: (1) reflective, (2) intermediate, (3) intermediate–dissipative, (4) dissipative, (5) rock platform-constrained, (6) non-barred dissipative and (7) dissipative.

the beachface. Our results show that the best predictions for beach states (Reflective, Intermediate and Dissipative domains) were obtained using the mean settling fall velocity of the subtidal sediments coupled to wave statistics one month prior to the field observation (Ω_o/Ω_p of 84.5%). When only storm waves (Hs > 2 m) are considered as the most relevant in generating morphological change, the Ωpredicted/Ωobserved ratios become very low, and only ratios for the berm are reasonably good (Ω_o/Ω_p of 60.7%). Ω is less skillful in predicting bar types (Intermediate domain). However, a reasonably good success rate of 72.3% is achieved when the subtidal sediment fall velocity is coupled to mean annual hydrodynamic conditions.

The results presented here highlight the relatively good skill of Ω in predicting large-scale variations in mean beach state, and provide very clear guidance on the importance of sediment sampling strategies and hydrodynamic conditions that need to be taken into account in a microtidal environment. Ω appears to be a better descriptor of beach states that do not change at the multi-decadal scale, than of bar types that can be subject to very dynamic short-term changes in the Gulf of Lions (Ferrer et al., 2009; Gervais et al., 2011), as in other low wave-energy environments (Hegge et al., 1996; Jackson et al., 2002; Costas et al., 2005; Gómez-Pujol et al., 2007). Thus, as aptly stated by Scott et al. (2011): "Beach classification models based on environmental parameters are, by necessity, simplifications and should be used as tools for understanding morphodynamic systems, rather than beach type prediction".

6. Conclusion

Nearly 200 km of sandy beach morphological state in the Gulf of Lions were investigated using 2D and 3D morphological surveying, sedimentological sampling and hydrodynamic monitoring. The large new data set obtained has enabled an analysis of the configuration and organization of the beach and associated bar types. It complements a prior review of the bar patterns in this microtidal Mediterranean setting (Aleman et al., 2011).

Our results show that:

- classical beach states described in the literature are present over the 200 km of the studied coast. Nevertheless, two unusual beach states for a microtidal environment (non-barred dissipative beaches and beaches constrained by a rock platform) are observed in relation to specific local environmental conditions.
- beach state transitions may be abrupt, depending on the disturbances caused by rock headlands, or continuous as a function of the alongshore sedimentary and hydrodynamic conditions.
- the geological framework has an important control on beach state. This control can be expressed by the presence of rocky barriers that are semi-impermeable to sediment transport (generating significant variability and sediment size families) or by the formation of sheltered beaches. In some compartments, bedrock outcrops limit accommodation space and lead to a decrease in wave energy. A net sediment deficit in the shoreface of the study area over the last 25 years has not affected the spatial and temporal persistence of identified beach states and bar types.
- the influence of harbours and smaller cross-shore engineering structures on the beach states appears to be insignificant.
- the parameter Ω has a level of predictive accuracy that strongly depends on specific wave periods and sediment sample locations. Prediction is best using average subtidal sediment statistics coupled to hydrodynamic conditions one month prior to observed beach state in a low-energy microtidal environment.

Acknowledgements

We thank the DREAL-LR for their financial support and the provision of LiDAR and hydrodynamic data. We also thank the entire team of the LITTOSIS campaign and the following people for the data collection in the course of previous field studies: P. Barthe, O. Beaurepaire, L. Cance, F. Carol, D. Cervello, C. Menniti, C. Michel, O. Raynal, R. Rivoal and M. Salvat. Frederic Bouchette (Géosciences-Montpellier), Heloïse Michaud (SHOM), two anonymous reviewers and Editor A. J. Plater for their helpful and constructive comments on the original draft. We acknowledge GLADYS (www.gladys-littoral.org) and SO LTC (www.soltc.org) research groups in regards to material support.

References

Akouango, E., 1997. Morphodynamique et dynamique sédimentaire dans le golfe du Lion. (Phd Thesis). Contribution à l'étude de la zone côtière dans l'actuel et le quaternaire récent. University of Perpignan, p. 191.
Aleman, N., 2013. Morphodynamique à l'échelle régionale d'une avant-côte microtidale à barres sédimentaires: le cas du Languedoc-Roussillon à l'aide de la technologie LiDAR. (PhD Thesis). University of Perpignan, p. 251.
Aleman, N., Certain, R., Robin, N., Barusseau, J.-P., 2015n. Influence of the Morphodynamic of Slightly Oblique Nearshore Bars on the Net Offshore Bar Migration (in preparation).
Aleman, N., Robin, N., Certain, R., Barusseau, J.P., Gervais, M., 2013. Net offshore bar migration variability at a regional scale: inter-site comparison (Languedoc-Roussillon, France). J. Coast. Res. (SI65), 1715–1720.
Aleman, N., Robin, N., Certain, R., Vanroye, C., Barusseau, J.P., Bouchette, F., 2011. Typology of nearshore bars in the Gulf of Lions (France) using LIDAR technology. J. Coast. Res. (SI64), 721–725.
Aloïsi, J.C., Got, H., Monaco, A., 1973. Carte géologique du précontinent languedocien au 1/250000ème, in: International Institute for Aerial Survey and Earth Sciences (I.T.C.), Netherlands.
Anfuso, G., Martinez del Pozo, J.A., Gracia, F.J., Lopez-Aguayo, F., 2003. Long-shore distribution of morphodynamic beach states along an apparently homogeneous coast in SW Spain. J. Coast. Conserv. 9, 49–56.
Anthony, E.J., 1998. Sediment-wave parametric characterization of beaches. J. Coast. Res. 14 (1), 347–352.
Backstrom, J.T., Jackson, D.W.T., Cooper, J.A.G., 2009. Contemporary morphodynamics of a high-energy headland-embayment shoreface. Cont. Shelf Res. 29 (11-12), 1361–1372.
Barusseau, J.-P., Radulescu, M., Descamps, C., Akouango, E., Gerbe, A., 1994. Morphosedimentary multiyear changes on a barred coast (Gulf of Lions, Mediterranean Sea, France). Mar. Geol. 122 (1–2), 47–62.
Barusseau, J.-P., Saint-Guily, B., 1981. Disposition, caractères et mode de formation des barres d'avant-côte festonnées du littoral du Languedoc-Roussillon (France). Oceanol. Acta 4 (3), 297–304.
Battjes, J.A., 1974. Surf similarity. 14th Conference on Coastal Engineering, pp. 466–480.
Bauer, B.O., Greenwood, B., 1988. Surf-zone similarity. Geogr. Rev. 78, 137–147.
Benaventes, J., Gracia, F.J., López-Aguayo, F., 2000. Empirical model of morphodynamic beachface behaviour for low-energy mesotidal environments. Mar. Geol. 167 (3–4), 375–390.
Benedet, L., Finkl, C.W., Campbell, T., Klein, A., 2004a. Predicting the effect of beach nourishment and cross-shore sediment variation on beach morphodynamic assessment. Coast. Eng. 51 (8–9), 839–861.
Benedet, L., Finkl, C.W., Klein, A.H.F., 2004b. Morphodynamic classification of beaches on the atlantic coast of florida: geographical variability of beach types, beach safety and coastal hazards. J. Coast. Res. (SI39), 360–365.
Brunel, C., Certain, R., Sabatier, F., Robin, N., Barusseau, J.P., Aleman, N., Raynal, O., 2014. 20th century sediment budget trends on the Western Gulf of Lions shoreface (France): an application of an integrated method for the study of sediment coastal reservoirs. Geomorphology 204, 625–637.
Calliari, L.J., Klein, A.H.F., Barros, F.C.R., 1996. Beach differentiation along the Rio Grande do Sul coastline (southern Brazil). Rev. Chil. Hist. Nat. 69, 485–493.
Casanobe, G., 1961. Pluviométrie, annales climatologiques. Chambre d'agriculture des P.O.pp. 11–16.
Castelle, B., Bonneton, P., Dupuis, H., Sénéchal, N., 2007. Double bar beach dynamics on the high-energy meso-macrotidal French Aquitanian Coast: a review. Mar. Geol. 245 (1–4), 141–159.
Cattaliotti-Valdina, D., 1978. Modalités et bilan de la sédimentation pélitique dans un milieu margino-littoral: le complexe lagunaire de Bages-Sigean-Port-la-Nouvelle. (PhD Thesis). University Paul Sabatier, Toulouse, p. 227.
Certain, R., 2002. Morphodynamique d'une côte sableuse microtidale à barres: le Golfe du Lion (Languedoc-Roussillon). University of Perpignan, p. 209.
Certain, R., Barusseau, J.-P., 2005. Conceptual modelling of sand bars morphodynamics for a microtidal beach (Sete, France). Bull. Soc. Geol. Fr. 176 (4), 343–354.
Certain, R., Meulé, S., Rey, V., Pinazo, C., 2005a. Wave transformation on a microtidal barred beach (Sète, France). J. Mar. Syst. 58 (1–2), 19–34.
Certain, R., Tessier, B., Barusseau, J.P., Courp, T., Pauc, H., 2005b. Sedimentary balance and sand stock availability along a littoral system. The case of the western Gulf of Lions littoral prism (France) investigated by very high resolution seismic. Mar. Pet. Geol. 22 (6–7), 889–900.
Cooper, J.A.G., Pilkey, O.H., 2004. Longshore drift: trapped in an expected universe. J. Sediment. Res. 74 (5), 599–606.
Costas, S., Alejo, I., Vila-Concejo, A., Nombela, M.A., 2005. Persistence of storm-induced morphology on a modal low-energy beach: a case study from NW-Iberian Peninsula. Mar. Geol. 224 (1–4), 43–56.
Cowell, P.J., Thom, B.G., 1994. Morphodynamics of coastal evolution. In: Carter, R.W.G., Woodroffe, C.D. (Eds.), Coastal Evolution: Late Quaternary Shoreline Morphodynamics. Cambridge Unviversity Press, Cambridge, pp. 33–86.

Davidson, M.A., Splinter, K.D., Turner, I.L., 2013. A simple equilibrium model for predicting shoreline change. Coast. Eng. 73, 191–202.
Dean, R.G., 1973. Heuristic Model of Sand Transport in the Surf Zone. Coastal Engineering, Sydney.
Durand, P., 1999. L'évolution des plages de l'ouest du Golfe du Lion au XXème Siècle: cinématique du traît de côte, dynamique sédimentaire, analyse prévisionnelle. (PhD Thesis). University Lumière of Lyon 2, p. 139.
Ferrer, P., Certain, R., Adloff, F., Bouchette, F., Barusseau, J.-P., Meulé, S., Robin, N., 2011. Hydrodynamics over a microtidal double crescentic barred beach in low energetic conditions (Leucate Beach, France). J. Coast. Res. (SI64), 2032–2036.
Ferrer, P., Certain, R., Barusseau, J.P., Gervais, M., 2009. Conceptual Modelling of a Double Crescentic Barred Coast (Leucate Beach, France). Coastal Dynamics, Tokyo, Japan, pp. 1–13.
Folk, R.L., Ward, W.C., 1957. Brazos River bar: a study in the significance of grain size parameters. J. Sediment. Petrol. 27 (1), 3–26.
Gervais, M., 2012. Impacts morphologiques des surcotes et vagues de tempêtes sur le littoral méditerranéen. (PhD Thesis). University of Perpignan, p. 399.
Gervais, M., Balouin, Y., Belon, R., 2012. Morphological response and coastal dynamics associated with major storm events along the Gulf of Lions Coastline, France. Geomorphology 143–144, 69–80.
Gervais, M., Balouin, Y., Thiébot, J., Certain, R., Bélon, R., Pedreros, R., Robin, N., Berne, S., 2011. Morphodynamic evolution of nearshore bars in response to winter storms (Lido de Sète, NW Mediterranean). J. Coast. Res. (SI64), 1855–1860.
Gibbs, R.J., Matthews, M.D., Link, D.A., 1971. The relationship between sphere size and settling velocity. J. Sediment. Petrol. 41 (1), 7–18.
Gómez-Pujol, L., Orfila, A., Cañellas, B., Alvarez-Ellacuria, A., Méndez, F.J., Medina, R., Tintoré, J., 2007. Morphodynamic classification of sandy beaches in low energetic marine environment. Mar. Geol. 242 (4), 235–246.
Grasso, F., Michallet, H., Barthélemy, E., Certain, R., 2009. Physical modeling of intermediate cross-shore beach morphology: transients and equilibrium states. J. Geophys. Res. 114 (C9001), 15.
Guizien, K., 2009. Spatial variability of wave conditions in the Gulf of Lions (NW-Mediterranean Sea). Life Environ. 59 (3-4), 261–270.
Guza, R.T., Inman, D.L., 1975. Edge waves and beach cups. J. Geophys. Res. 80 (21), 2997–3012.
Hegge, B., Elliot, I., Hsu, J., 1996. Sheltered sandy beaches ofsouthwestern Australia. J. Coast. Res. 12 (3), 748–760.
Jackson, D.W.T., Cooper, J.A.G., 2009. Geological control on beach form: accommodation space and contemporary dynamics. J. Coast. Res. (SI56), 69–72.
Jackson, D.W.T., Cooper, J.A.G., del Rio, L., 2005. Geological control of beach morphodynamic state. Mar. Geol. 216 (4), 297–314.
Jackson, N.L., Nordstrom, K.F., Eliot, I., Masselink, G., 2002. "Low energy" sandy beaches in marine and estuarine environments: a review. Geomorphology 48, 147–162.
Jiménez, J.A., Guillén, J., Falqués, A., 2008. Comment on the article "Morphodynamic classification of sandy beaches in low energetic marine environment" by Gómez-Pujol, L., Orfila, A., Cañellas, B., Alvarez-Ellacuria, A., Méndez, F.J., Medina, R. and Tintoré, J. Marine Geology, 242, pp. 235–246, 2007. Mar. Geol. 255 (1–2), 96–101.
Klein, A.H.F., Ferreira, Ó., Dias, J.M.A., Tessler, M.G., Silveira, L.F., Benedet, L., Menezes, J.T., De Abreu, J.G.N., 2010. Morphodynamics of structurally controlled headland-bay beaches in southeastern Brazil: a review. Coast. Eng. 57, 98–111.
Klein, A.H.F., Menezes, J.T., 2001. Beach morphodynamics and profile sequence for a headland bay coast. J. Coast. Res. 17 (4), 812–835.
L.C.H.F., 1984. La côte méditerranéenne, de la frontière espagnole à la frontière italienne. Catalogue sédimentologique des côtes de France, Parisp. 426.
Levoy, F., Anthony, E., Barusseau, J.-P., Howa, H., Tessier, B., 1998. Morphodynamique d'une plage macrotidale à barres. Comptes Rendus de l'Académie des Sciences — series IIA. Earth Planet. Sci. 327 (12), 811–818.
Lippmann, T.C., Holman, R.A., 1990. The spatial and temporal variability of sand bar morphology. J. Geophys. Res. 92 (C7), 11575–11590.
Loureiro, C., Ferreira, Ó., Cooper, J.A.G., 2013. Applicability of parametric beach morphodynamic state classification on embayed beaches. Mar. Geol. 346, 153–164.
Masselink, G., Short, A.D., 1993. The effect of tide range on beach morphodynamics and morphology: a conceptual beach model. J. Coast. Res. 9 (3), 785–800.
Mayençon, R., 1992. In: Edilarge, S.A. (Ed.), Météorologie marine. Imp. Maury.
Michel, C., Aleman, N., Robin, N., Certain, R., Guerinel, B., Vanroye, C., Barusseau, J.P., Bouchette, F., 2011. Modification des configurations de barres d'avant-côte au voisinage des ports de plaisance: exemple du Languedoc-Roussillon. 13ème Congrès Français de Sédimentologie. ASF, Dijon, p. 342.
Montreuil, A.-L., Levoy, F., Bretel, P., Anthony, E.J., 2014. Morphological diversity and complex sediment recirculation on the ebb delta of a macrotidal inlet (Normandy, France): a multiple LiDAR dataset approach. Geomorphology 219, 114–125.
Muñoz-Perez, J.J., Medina, R., 2010. Comparison of long-, medium- and short-term variations of beach profiles with and without submerged geological control. Coast. Eng. 57 (3), 241–251.
Person, R., 1973. Contribution à l'étude thermique du Golfe de Lion. (PhD Thesis). University of Paris VI, p. 115.
Price, T.D., Ruessink, B.G., 2011. State dynamics of a double sandbar system. Cont. Shelf Res. 31 (6), 659–674.
Ranasinghe, R., Symonds, G., Black, K., Holman, R., 2004. Morphodynamics of intermediate beaches: a video imaging and numerical modelling study. Coast. Eng. 51 (7), 629–655.
Robin, N., Certain, R., Bouchette, F., Anthony, E.J., Meulé, S., Aleman, N., 2014. Wave-driven circulation over a double nearshore bar system during storm conditions. J. Coast. Res. (SI70), 84–89.
Sabatier, F., Stive, M.J.F., Pons, F., 2004. Longshore variation of depth of closure on a microtidal wave-dominated coast. International Conference of Coastal Engineering, Lisboapp. 2327–2339.
Sanderson, P.G., Eliot, I., 1999. Compartmentalisation of beachface sediments along the southwestern coast of Australia. Mar. Geol. 162, 145–164.
Saye, S.E., van der Wal, D., Pye, K., Blott, S.J., 2005. Beach–dune morphological relationships and erosion/accretion: an investigation at five sites in England and Wales using LIDAR data. Geomorphology 72 (1–4), 128–155.
Scott, T., Masselink, G., Russell, P., 2011. Morphodynamic characteristics and classification of beaches in England and Wales. Mar. Geol. 286 (1–4), 1–20.
Scott, T., Russell, P., Masselink, G., Wooler, A., Short, A.D., 2007. Beach rescue statistics and their relation to nearshore morphology and hazards: a case study for Southwest England. J. Coast. Res. (SI50), 1–6.
Sénéchal, N., Gouriou, T., Castelle, B., Parisot, J.P., Capo, S., Bujan, S., Howa, H., 2009. Morphodynamic response of a meso- to macro-tidal intermediate beach based on a long-term data set. Geomorphology 107 (3–4), 263–274.
Short, A.D., 1991. Macro-meso tidal beach morphodynamics — an overview. J. Coast. Res. 7 (2), 417–436.
Short, A.D., 1992. Beach systems of the central Netherlands coast: processes, morphology and structural impacts in a storm driven multi-bar system. Mar. Geol. 107 (1–2), 103–132.
Short, A.D., 1999. Handbook of Beach and Shoreface Morphodynamics. Wiley.
Short, A.D., 2006. Australian beach systems — nature and distribution. J. Coast. Res. 22 (1), 11–27.
Short, A.D., 2010. Role of geological inheritance in Australian beach morphodynamics. Coast. Eng. 57 (2), 92–97.
Short, A.D., Aagaard, T., 1993. Single and multi-bar beach change models. J. Coast. Res. (SI15), 141–157.
Short, A.D., Jackson, D.W.T., 2013. Beach morphodynamics. In: Shroder, J.F. (Ed.), Treatise on Geomorphology. Elsevier, Academic Press, Amsterdam, San Diego, pp. 106–129.
Short, A.D., Woodroffe, C.D., 2009. The Coast of Australia. Cambridge University Press, Melbourne.
Shrestha, R.L., Carter, W.E., Sartori, M., Luzum, B.J., Slatton, K.C., 2005. Airborne Laser Swath Mapping: quantifying changes in sandy beaches over time scales of weeks to years. ISPRS J. Photogramm. Remote Sens. 59 (4), 222–232.
Splinter, K.D., Turner, I.L., Davidson, M.A., Barnard, P., Castelle, B., Oltman-Shay, J., 2014. A generalized equilibrium model for predicting daily to interannual shoreline response. J. Geophys. Res. Earth Surf. 119 (9), 1936–1958.
Sunamura, T., Horikawa, K., 1974. Two-dimensional beach transformation due to waves. In: ASCE (Ed.), 14th International Conference in, Coastal Engineering, pp. 920–938.
Sunamura, T., Takeda, I., 1984. Landward migration of inner bars. Mar. Geol. 60 (1–4), 63–78.
Thieler, E.R., Pilkey, O.H., Cleary, W.J., Schwab, W.C., 2001. Sedimentation on the shoreface and inner continental shelf at Wrightsville beach, North Carolina, U.S.A. J. Sediment. Res. 71 (6), 958–970.
Vanroye, C., 2009. Evolution des pratiques de suivi topo-bathymetrique du littoral en Languedoc-Roussillon: l'utilisation du lidar, Conférence Méditerranéenne Côtière et Maritime. Hammamet, Tunisie, pp. 311–314.
Vousdoukas, M., Velegrakis, A., Karambas, T., Valais, G., Zarkogiannis, S., 2005. Morphodynamics of Beachrock Infected Beaches: Vatera Beach, Northeastern Mediterranean, Coastal Dynamics. pp. 1–14.
Wright, L.D., Kim, C.S., Hardaway, C.S., Kimball, S.M., Green, M.O., 1987. Shoreline and Beach Dynamics of the Coastal Region From Cape Henry to False Cape, Technical Report. Virginia Institut of Marine Science, p. 116.
Wright, L.D., Short, A.D., 1984. Morphodynamic variability of surf zones and beaches: a synthesis. Mar. Geol. 56 (1–4), 93–118.
Wright, L.D., Short, A.D., Green, M.O., 1985. Short-term changes in the morphodynamic states of beaches and surf zones: an empirical predictive model. Mar. Geol. 62 (3–4), 339–364.
Wright, L.D., Thom, B.G., 1977. Coastal depositional landforms: a morphodynamic approach. Prog. Phys. Geogr. 1 (3), 412–459.